Universidade Católica Portuguesa
Faculdade de Engenharia

Applicability of the Statistical Pattern Recognition Paradigm for Structural Health Monitoring of Bridges

João Tiago Martins Neves Pereira

Dissertação para obtenção do Grau de Mestre em Engenharia Civil

Júri

Prof. Doutor Manuel José Martinho Barata Marques, Chair
Prof. Doutor Luis Armando Canhoto Neves
Prof. Doutor Elói João Faria Figueiredo, Advisor

September 2012

TABLE OF CONTENTS

LIST OF FIGURES

LIST OF TABLES

NOTATION

All the symbols used in this dissertation are defined when they first appear in the text. For the reader's convenience, this section contains the meanings of the commonly used acronyms and symbols.

Abbreviations

AIC	Akaike's Information Criterion
AR	Autoregressive
AR (p)	Autoregressive model of order p
BMS	Bridge Management System
DAQ	Data Acquisition
DI	Damage Indicator
DOF	Degree of Freedom
EM	Expectation-Maximization
EP	Estradas de Portugal S.A.
FHWA	Federal Highway Administration
FEM	Finite Element Model
FOS	Fiber Optic Sensors
GMM	Gaussian Mixture Models
GPS	Global Positioning System
LANL	Los Alamos National Laboratory
LVDT	Linear Variable Differential Transducers
MSD	Mahalanobis Squared Distance
ML	Maximum Likelihood
NBI	National Bridge Inventory

NDT	Non-destructive Testing
NBIS	National Bridge Inspection Standards
NTSB	National Safety and Transportation Board
PDF	Probability Density Function
RSS	Residual Sum of Squares
SHM	Structural Health Monitoring
SOFO	Surveillance d'Ouvrages par Fibres Optiques
SPR	Statistical Pattern Recognition
USA	United States of America

Roman Symbols

c	Threshold value
D	Mahalanobis distance
e	Residual error value
m	Feature vector dimension
n	Number of observations
p	Model order
s	Measured signal (or response time series)
$\mathbf{s}$	Vector of measured signals
$\mathbf{x}$	Feature vector
$\mathbf{X}$	Matrix of feature vectors from the training data
$\mathbf{z}$	Feature vector
$\mathbf{Z}$	Matrix of feature vectors from the test data

w	Mixture weight

Greek Symbols

α	Level of significance
ε	Sum-of-square of errors
$\boldsymbol{\mu}$	Mean vector
$\boldsymbol{\Sigma}$	Covariance matrix
λ	Gaussian mixture model parameters
ϕ	Vector of auto-regressive parameters
χ_m^2	Central chi-square distribution with m degrees of freedom

ABSTRACT

In the last decades, health monitoring systems have gained an increasing importance in our society. The main purpose of these systems is to support the engineers to get more insight into the behavior of structures under service conditions, so they can optimize and improve maintenance programs and, hopefully, to avoid structural failures or disasters. It is possible to integrate these systems in any type of civil or mechanical infrastructure. However, in this dissertation, the preferential targets are the civil infrastructures with major strategically importance in the social environment, such as bridges and viaducts.

Therefore, the goal of this dissertation is (i) to review the most recent bridge collapses in order to unveil the main causes and challenges posed by those catastrophic events; (ii) to review the concept and need of Structural Health Monitoring (SHM) of bridges as well as its associated potential for significant life-safety and economic benefits; and (iii) to study the applicability of the SHM concepts. Due to recent promising research developments, the SHM process is posed in the context of the Statistical Pattern Recognition (SPR) paradigm, which tries to implement a damage identification strategy based on the comparison of different state conditions.

The applicability of the SHM-SPR paradigm is studied by applying its concepts in two separate cases: firstly on data sets from a base-excited three-story frame structure, created and tested in a laboratory environment at Los Alamos National Laboratory; secondly, on data sets from a real-world bridge, namely the Z24 Bridge in Switzerland.

The major contributions of this dissertation are the extension of previous results obtained by Figueiredo et al. from the three-story frame structure and the development and application of an algorithm that uses a Gaussian mixture model as a way of improving the feature classification performance under varying operational and environmental conditions.

Keywords: Damage Detection; Bridge Failures; Statistical Pattern Recognition Paradigm; Structural Health Monitoring.

RESUMO

Nas últimas décadas, os sistemas de monitorização estrutural ganharam uma crescente importância na nossa sociedade. O principal objetivo destes sistemas é de ajudar os engenheiros a aprofundar o conhecimento relativo ao comportamento das estruturas sob condições de serviço para que possam otimizar e melhorar os programas de manutenção e, em último caso, evitar desastres ou falhas estruturais. É possível integrar estes sistemas em qualquer tipo de infra-estrutura civil ou mecânica. No entanto, nesta dissertação, os alvos preferenciais são as infra-estruturas com elevada importância estratégica no seio da engenharia civil, tais como as pontes e os viadutos.

Portanto, o objetivo desta dissertação é (i) rever os recentes colapsos de pontes, de forma a desvendar as causas que os originaram assim como os desafios colocados por estes eventos; (ii) rever o conceito e a necessidade de sistemas de monitorização da integridade estrutural (SHM) de pontes, bem como o seu potencial associado aos benefícios ao nível da segurança e do ponto de vista económico; e (iii) estudar a aplicabilidade dos conceitos da SHM. Devido a recentes desenvolvimentos promissores, o processo de SHM pode ser colocado no contexto de um paradigma de reconhecimento de padrões (SPR), o qual tenta implementar uma estratégia de identificação de dano com base na comparação de diferentes estados de condição da estrutura.

A aplicabilidade do paradigma SHM-SPR é estudada através da aplicação dos seus conceitos em dois casos distintos: em primeiro lugar, em conjuntos de dados recolhidos de uma estrutura de três pisos, criada e testada em ambiente laboratorial no Los Alamos National Laboratory; em segundo lugar, em conjuntos de dados de uma ponte real, mais especificamente, a Ponte Z24, na Suíça.

As contribuições originais desta dissertação são a extensão dos resultados anteriormente obtidos por Figueiredo et al. relativos à estrutura de três pisos, e o desenvolvimento e aplicação de um algoritmo, que utiliza como base um modelo de mistura Gaussiana, de forma a melhorar o desempenho da classificação de características sob condições operacionais e ambientais variáveis.

Palavras-Chave: Deteção de Dano, Desastres de Pontes; Paradigma de Reconhecimento de Padrões; Monitorização da Integridade Estrutural.

ACKNOWLEGMENTS

First and foremost I would like to express my deep gratitude to my advisor, Elói Figueiredo, for his support and guidance throughout the course of this thesis. I thank him for giving me his time, sharing his scientific knowledge and for giving me all resources needed to accomplish this work.

I also wish to thank my close friends and family, who have helped me stay sane through these times. I deeply value their friendship and appreciate their belief in me. I wish to thank Jorge in particular for all his help during this period. Most importantly, I wish to thank Ana for her personal support, endless patience and encouragement when it was most required.

Finally, I thank my parents for supporting me throughout all my studies at University and for giving me the love and guidance to overcome every challenge. They are my role models.

.

1. INTRODUCTION

Throughout the history, the civil engineering has had a key role in our society. It is nearly impossible to imagine the modern society without bridges, railways, dams, tunnels, roads, nuclear stations, power plants, hospitals, or even schools. Unfortunately during their service period, that can go from decades to over hundred years, this infrastructure ages and deteriorates. These aging and deteriorating processes can often lead to the loss of material properties, which can compromise the ability of the infrastructure to perform its main purpose, or ultimately it can lead to structure failures. Therefore, it is crucial for the owner/operator of the infrastructure to have valid and reliable information regarding the extent of the damage/deterioration and how it will affect the remaining service-life and capacity of the structures, so that a well-informed decision can be made regarding its repair. In the last decades, intelligent health monitoring systems have increasingly become an important technology that attempts to provide knowledge about the actual condition of a structure, allowing an optimal use of the structural members, drastically changes in the organization of maintenance services, minimized downtime for maintenance, and the avoidance of catastrophic failures. The ability to permanently determine the condition of the structure allows decisions to be made in real time instead of being planned years ahead by following the empirical manuals. Thus, those systems have the potential to allow the maintenance plans to evolve from a time-based schedule to condition-based maintenance. Therefore, in the particular case of the bridges and in order to understand the need of monitoring systems, Chapter 2 is concerned with the description of the most recent bridge collapses to unveil the main causes, the lessons learnt from them, the measures taken to prevent future disasters, and the challenges and the developments posed by those catastrophic events.

Despite all the developments on the Bridge Management Systems (BMSs) and the visual-inspections-based tools, the need for better structural condition assessment methodologies has pushed the scientific community to the implementation of a damage identification strategy, which is referred to as Structural Health Monitoring (SHM) [1]. Generally, the SHM process requires the definition of potential damage scenarios of a system, the observation of that system for a given period of time using periodically spaced measurements, extraction of damage-sensitive features from those measurements, and analysis of those features in order to determine the current structural state condition. In long term, the output of this process is periodically updated information concerning the ability of the structure to perform its function by taking into account its aging and degradation resulting from operational environments. Currently, the feature analysis can be done in two different but

complementary approaches. The first one is to use physics-based models, where the structure is modeled using a traditional finite element model (FEM). Then, the model is periodically updated based on information from the measured data. This procedure is also known as inverse problem. The second one, and extensively demonstrated in this dissertation, is to use the so-called data-based models, where statistical models (such as machine learning algorithms) are developed to learn the normal condition of the structures from the measured data. This approach intends to eschew complex FEM models and, therefore, pave the way for data-based models applicable to systems of arbitrary complexity. In the end, some sort of pattern recognition may be used to detect the presence of damage in the structures. Therefore, in Chapter 3, the SHM process is posed in the context of a Statistical Pattern Recognition (SPR) paradigm, which can be broken down into a four-stage process: (1) Operational Evaluation, (2) Data Acquisition (3) Feature Extraction, and (4) Statistical Modeling for Feature Classification. Additionally, this chapter points out the economic and safety considerations of this concept as well as several limitations and challenges for implementing an effective SHM system. Especially, the influence of the operational and environmental variability is highlighted. Actually, the separation of changes in sensor readings caused by damage from those caused by changing operational and environmental conditions is one of the biggest challenges for transitioning SHM technology from research to practice [2].

Finally, in order to demonstrate the applicability of the SPR paradigm, Chapter 4 tests and applies the described statistical procedures on standard data sets from a base-excited three-story frame structure under simulated operational and environmental conditions. To the extent possible, all SHM technology should be validated using data from real-world structures. Thus, in Chapter 5 the SPR paradigm is applied on vibration data from the Z24 Bridge, in Switzerland. The real-world data sets are unique in the sense that they combine one-year monitoring with realistic damage scenarios (such as settlements, spalling of concrete, failure of a concrete hinge, failure of anchor heads, and failure of tendon wires) and effects of the operational and environmental variability [3].

1.1. Objective and Original Contributions of this Dissertation

The objective of this dissertation is to review the concept and need of SHM of bridges and its potential for significant life-safety and economic benefits. Additional, it intends to test the applicability of several SPR techniques for damage detection and localization on data sets from a laboratory structure and for damage detection on data sets from a real-world bridge - the Z24 Bridge.

While the data sets from the laboratory structure has been extensively used for damage detection [2,4], in this dissertation those data sets are used to step forward in the hierarchy of damage identification [5], namely for damage localization, which stands as a significant contribution to the SHM field. Additionally, the applicability of the SPR paradigm on the data sets from the Z24 Bridge permitted to develop and apply Gaussian mixture models (GMM) for damage detection under varying operational and environmental conditions. Actually, these models demonstrated to be useful for real-world applications, as it permits to separate nonlinear changes in the sensors readings caused by environmental conditions from changes caused by real-world damage scenarios.

2. FROM BRIDGE FAILURES TO SHM APPLICATIONS

Among all civil engineering infrastructures, bridges attract the greatest attention within the engineering community due to their small safety margins and their great exposure to the public. For centuries the mankind has relied on the transportation systems, even ancient civilizations such as the Romans or the Incas used bridges as the backbone of their empires. For instance, in the city of Chaves, northern Portugal, the Roman Bridge, built in the first century AD, still carries normal traffic (Figure 2-1) [6].

Nowadays the quality and efficiency of transportation infrastructure is an important component in the country's economy. For instance, by 2012, a Portuguese road concessionary, Estradas de Portugal S.A. (EP), has in its inventory system, approximately, 5000 bridges [7]. Apart from their utility, bridges are also landmarks admired for their great esthetic impact [8] such as the Golden Gate Bridge, in San Francisco, California, and the 25 de Abril Bridge, in Lisbon, Portugal.

Figure 2-1: Roman Bridge in Chaves, Portugal.

This chapter intends to summarize the main causes of bridge failures in the recent decades, the main SHM real applications on bridges, in order to understand how these systems are prepared to avoid future failures.

2.1. Typical Causes of Bridge Failures

It is well-known that learning from the past, helps to understand the present and create the future. Therefore, the study and analysis of past failures is an important task to understand the conditions that brought about these failures and finding ways to avoid them is a crucial step

in order to minimize future life losses. If interpreted correctly, failures can produce a fair amount of information that can, for instance, help to better understand the bridge performance, trigger the development of a particular bridge concept, increase knowledge regarding certain phenomenon or material strengths, which can ultimately lead to the development of more efficient design codes. Actually, it is always better to avoid failures through an appropriate design rather than to rely on a SHM system.

Bridge failures can be a result of a great number of factors. Even though it is not possible to create a complete and accurate list of all bridge failures throughout history, as some are not well documented, the majority of those cases have been reported as a result of natural events, human errors, and deterioration caused by aging.

There are a vast number of cases caused by natural events. It has been estimated that more than half of all bridge failures are a result of hydraulic-related causes, such as floods and scour. Scour can be defined as the removal of bank material from around the bridge abutment or pier foundations due to flowing water. Actually, it has been reported as the most common cause of bridge failures in the United States of America (USA) [8]. This process reduces the capacity of existing foundations, compromising the integrity of the structure and, when not monitored, it can lead to its collapse. The Hintze Ribeiro Bridge, in Portugal, stands as one of the most famous cases of bridge collapses due to scour as will be later on discussed in Subsection 2.2.

Another major cause of bridge failures, mainly because of its devastation rather than its high level of occurrence, is the earthquake event. During these events, which usually last for more than a few seconds, considered damage can occur with bridge structures when they are not prepared to undertake the seismic actions. Nowadays almost every civil engineering infrastructure has to be built taking into account seismic activity. The I-10 Freeway, in Los Angeles, is one out of many examples of earthquake-related damage in bridges, which suffered severe damage during the 1994 earthquake in Northridge, California.

Failures due to wind are also a main natural cause of bridge collapses. Wind plays a very important role when designing a bridge because it evokes a dynamic response from structures exposed to it. This dynamic response comes in the form of vibration actions in resonance with bridge's natural frequencies of vibration. High-speed winds, such as tornados, can also be a cause for bridge disasters. The Takoma Narrows suspension bridge, that used to link the Olympic Peninsula with the rest of the state of Washington, still stands as the most renowned bridge collapse due to wind action.

In some countries there is a chance of floating ice damage. Depending on the size of the river, the speed of the current, and the size of the ice blocks, their collision with the bridge piers can produce the same effect as an impact from a moving vehicle. In these cases, timber fenders should be built in order to shield the piers.

Human errors also play a major part when it comes to bridge failures. Failures due to human error represent some of the biggest disasters through history, with a variety of causes that can go from design and/or construction deficiency, lack of maintenance, fire, terrorist attacks, and collisions [9]. The collisions are related to vehicle, train, or vessel impacts. Vehicle impacts occur mainly because many older bridges do not have the minimum clearance required by the current codes, resulting in heavy truck collisions that can cause serious damage to the bridge. Vehicle collisions can also be linked to fire damage, as a consequence of overturning trucks that may leak gasoline and catch fire [9]. Even though vehicle collisions have a high occurrence frequency, vessel collisions have a higher mortality rate. Two of the most famous disasters regarding vessel impacts were the Sunshine Skyway Disaster (Figure 2-2) in Florida and the I-40 Bridge Disaster (Figure 2-2) in Oklahoma, in the USA [10, 11]. The first happened in 1980 when a freighter collided with a pier during a storm, taking down over 350m of bridge. The collision caused ten cars and a bus to fall in the water, killing 35 people. The second happened in 2002 when a tugboat collided with a bridge support causing the fall of a section of the bridge. This accident caused the death of 14 people. Design deficiencies often happen when assumptions made during the designing process do not represent the behavior of the superstructure in the field. The I-35W Bridge, Minneapolis, is one recent failure caused by design deficiencies (more details in Subsection 2.2).

Figure 2-2: Sunshine Skyway disaster, Florida, USA (on the left); I-40 Bridge disaster, Oklahoma, USA (on the right).

Bridge failures are encountered not only on the field but also on construction sites. The construction stage of a bridge is its most vulnerable stage. It is during construction that, sometimes, critical items are overlooked leading to failure. Some examples of failures during construction are: under-designed temporary support elements, inadequate scaffolding, executed construction sequence different from the one planned, or even use of wrong bolts. The lack of maintenance is, unfortunately, also responsible for bridge failures. The constant increase of traffic with more and heavier trucks on our highways, increasing the rates of deterioration of bridges and pavements, combined with the fact that some older bridges were not designed accordingly to the design criterion of today, makes periodic inspections an essential task in order to prevent bridge failures [9].

Finally, the natural aging and deterioration of the bridges is a factor that needs to be taken into account within the main causes of bridge failures. Bridges, like all civil infrastructures, have a service-life as a result of the deterioration that the bridge materials will suffer along the years. Although bridge aging alone is not the main cause of bridge failures, mainly because of the periodically visual inspections throughout its service-life, it is not an aspect that can be taken lightly or overlooked when talking about bridge failures. Most failures due to aging and deterioration are associated with lack of maintenance and neglect but they can also be a result of new codes and regulations that the structure cannot meet, most likely regarding capacity loads.

2.2. Analysis of Recent Bridge Failures

Over recent decades, more attention has been given to the condition assessment of bridges. In the USA, the first need came up in 1967 with the collapse of the Silver Bridge that used to connect the states of West Virginia and Ohio (Figure 2-3) [12]. On December 15, at approximately 5pm, the bridge suddenly collapsed into the Ohio River during the rush hour, resulting in the deaths of 46 people. After investigating the wreckage, conclusions pointed out that the cause of the collapse was the failure of an eyebar as a result of a small defect, which caused very high tensile stress. Additionally, the location of the defective bar was not accessible by visual inspection. At the time of construction (1928), planners were still inexperienced in the effects of conditions known as stress corrosion and stress fatigue. However, the types of structural corrosion, which caused the cracks and subsequent collapse of the Silver Bridge, would be undetectable even with the means at our disposal today. Only by disassembling the joint itself would be possible to notice the flaw, which is not realistic once the bridge is completed [12, 13].

Figure 2-3: Silver Bridge collapsed, Ohio, USA.

This tragic collapse sparked a national interest in the safety inspection and maintenance of older bridges, which led, in 1971, the Federal Highway Administration (FHWA) to create the National Bridge Inspection Standards (NBIS). The NBIS established national policy regarding inspection procedures, frequency of inspections, and qualifications of personnel among others. Bridges were required to be inspected every five years, with the exception of important structures that were to be inspected within a two-year interval.

Despite the nationwide inspection procedures brought about by the Silver Bridge Disaster, aging infrastructures were still a problem in the USA. In 1983, a section of the Mianus River Bridge in Greenwich, Connecticut, collapsed completely separating from the bridge and falling into the river. This incident resulted in three deaths and three serious injuries. After an investigation, performed by the National Safety and Transportation Board (NSTB), the cause of the collapse was pointed as a result of corrosion due to inadequate drainage. However, it was also indicated that the inspection progress was not thorough enough. The number of inspectors in the state was significantly low when compared to the amount of bridges used daily. Furthermore, there was no equipment available to check major stress points on the bridge and, to make matters worse, some inspectors even signed off without performing an inspection. After this incident more inspectors were hired and new inspection procedures were established, however accidents due to lack of maintenance or neglect and design deficiency continued to happen [14].

With the collapse of the I-90 at Schoharie Creek, in New York, in April 1987, attention was turned to underwater inspection. This disaster, which took the lives of ten people, occurred during the spring flood when two spans of the bridge fell into the river after a pier, which supported the spans, collapsed due to scour damaged. Shortly after the first collapse, the waters

brought down another pier and span. This second collapse was a result of the first one, which had blocked the stream flow diverting the flooding waters towards the second pier, who toppled due to the increased velocity and amount of water [15]. In Figure 2-4 is possible to visualize the result of scour damage in one of the piers [16].

Figure 2-4: Scour at I-90 West Pier.

The NTSB concluded that the bridge footings were susceptible to scour as a result of poor riprap around the base of the piers and a shallow foundation. This collapse brought attention to the vulnerability of bridges failures due to scour, since approximately 86% of the 593,000 bridges in the National Bridge Inventory (NBI) were over waterways. As a result, the FHWA introduced revisions on design, maintenance, and inspection to their guidelines [17].

In 2007, the collapse of the I-35W Bridge (Figure 2-5) over the Mississippi River in Minneapolis, Minnesota, brought once again bridge safety to the forefront of the public [18]. The disaster occurred during evening rush hour causing 13 deaths and 145 injuries. The bridge had been inspected annually since 1993 and, before that, used to be inspected every two years, as mandated by the NBIS. Furthermore, in the years previous to the collapse, the bridge was rated as "structurally deficient", due to the load paths in the structure being non-redundant, meaning that a failure of any one of a number of structural elements in the bridge would result in a complete collapse of the entire bridge [19].

Figure 2-5: I-35W Bridge collapsed, Minnesota, USA.

The NSTB report concluded that the problem behind the collapse was a design error that resulted in some gusset plates being undersized and not able to carry the load that was placed on the bridge. The renovations taking place at the time of the collapse made matters worse. The increased concrete deck (from 6.5 inches to 8.5 inches), center median and outside barrier walls, and the fact that all machinery and paving materials were being parked and stockpiled on the center span added considerably to the overall weight of the structure. The undersized gusset plates combined with the additional load of the renovations and the rush hour traffic caused the bridge to collapse into the Mississippi River [9].

In China, a wide range of bridge failures can also be pointed as a motivation for the developments in codes and regulations, as well as the maintenance programs updates for this kind of infrastructure. One of the most famous failures was the Qijiang Rainbow Bridge, a pedestrian bridge that in 1999 collapsed after a short three-year service period, resulting in 40 deaths and 14 injuries. Further investigation concluded that the collapse was a result of the inferior quality steel used in its construction that led to the early development of rust, as well as weak concrete and poor welding [20]. Other cases like the 2006 Liaoning Yingkou Xiongyue Brigde failure due to scour damage in the piers [21] or the recent collapse of a bridge in Changchun [22] where the bridge concrete slab simply collapsed under a passing truck, still shine light on the importance of developing SHM systems in order to prevent these types of disasters.

In Portugal, it was only after the Hintze Ribeiro Bridge disaster (Figure 2-6) that authorities became more concerned about the aging of bridges [23]. This disaster occurred on March 4th, 2001, when one of the bridge piers collapsed killing 59 people, as occupants of a bus and three cars crossing the bridge at the time. The illegal sand extraction, which compromised

the stability of the bridge's piers (as well as disregard from the responsible officials despite of the warnings of divers and technicians), was pointed out as the main cause of the collapse. A global campaign of bridge inspections was set into motion, with a total of almost 350 inspections, as a reaction to the incident. In consequence, and as a result of those inspections, three bridges were immediately closed and in 56 bridges were imposed loadings and velocity restrictions [24]. Currently, EP have adopted a multi-year routine-inspection plan. This plan consists of main underwater inspections performed every four years in, approximately, 150 bridges with foundations permanently under water. Additionally, these inspections are carried out in a two-year cycle for flagged cases [7].

Figure 2-6: Hintze Ribeiro Bridge disaster, Portugal.

Note that although this incident alerted authorities to the importance of bridge inspection and maintenance, SHM systems had already started being used a couple of years back with the construction, for instance, of the Vasco da Gama Bridge (more details in Subsection 2.3).

In the rest of the world, similar disasters have taken place over the years. On October 21st, 1994, with the collapse of the Seongsu Bridge, Seoul, South Korea, 32 people died and 17 people were injured. Joints of trusses supporting the bridge slab, which were not completely welded, caused the failure. The welding thickness, which should be approximately 10 millimeters, was only 8 millimeters. Additionally, the connecting pins for steel bolts were of poor quality. After the incident the bridge was closed for repair, however, due to its poor construction it had to be completely redesigned and rebuilt [25]. In Spain, on November 7th, 2005, due to a design error, three of the piers of the Motorway Bridge at Almuñecar, Granada, collapsed, causing a 60 meter section of the bridge to fall from a height of 80 meters onto workers below causing 6 deaths and 3 injuries [26]. In India, on August 28th, 2003, a bridge in

Daman collapsed as a consequence of severe damage caused by violent rainstorm. Over 25 people were killed, including over 20 children who were on their way back home from school. The lack of maintenance and repair were appointed as a contributing cause of the disaster [26]. Three years later, another disaster took place in India, when a 150-year-old footbridge, in Bihar, suddenly collapsed over a train passing beneath it, killing 33 people. At the time of collapse the bridge was being dismantled [26].

2.3. Bridge Management Systems

In a response to the many bridge disasters, most bridge owners around the world have adopted the so-called BMSs to build inventories and inspection history databases. These systems are essentially visual-inspection-based decision-support tools developed to analyze engineering and economic factors and to assist the authorities in determining how and when to make decisions regarding maintenance, repair, and rehabilitation of structures in a systematic way [2]. In the early 1990s several software packages were developed to assist in managing bridges, such as PONTIS and BRIDGIT in the USA, DANBRO in Denmark [27], and GOA in Portugal [28].To date, the structural condition assessment of these systems essentially relies on weighted indices based on visual inspections and/or preliminary Non-destructive Testing (NDT) technologies. More details about these systems can be found in the references [29].

2.4. SHM Applications

The current practice of visual inspection associated with the BMS has been identified as a shortcoming in condition assessment. At the 50th anniversary of the Interstate Highway System, Walther and Chase [30] stated that despite the advances in BMS modeling, the condition assessment activities associated with NBIS and BMS still rely heavily on visual inspections, which inherently produces widely variable results. The same authors stressed that the challenge would be to develop better assessment methodologies that can generate better prediction models to support the owners' decisions regarding bridge safety assessment and maintenance.

After several developments of BMS modeling, the failures mentioned in the Subsection 2.2 were the stepping-stone to a better awareness in terms of structural condition assessment. Therefore, these disasters, along with the limitations posed by the visual inspections, brought forward the motivation for the real-world field SHM applications. In the USA, after de collapse of the I-35W Bridge, a new bridge was built in its place. The new I-35W Saint Anthony Falls Bridge is an excellent example of a truly integrated SHM system, combining different sensing

technologies in order to monitor the bridge performance and aging behavior. The rebuilt I-35W demonstrated that a high level of safety can be attained not only during construction, but also throughout the estimated 100-year life-span of the bridge. The system implemented includes a range of sensors capable of measuring various parameters to enable the bridges behavior to be monitored. Local static strains, curvatures, concrete creep, and shrinkage are measured by strain gauges; ambient temperature, temperature gradient, and thermal strain are measured by thermistors; and joint movements are measured by linear potentiometers. Accelerometers were placed at the mid-spans in order to measure traffic-induced vibrations and modal frequencies. There were also installed corrosion sensors to measure the concrete resistivity and corrosion, as well as SOFO (French acronym of Surveillance d'Ouvrages par Fibres Optiques) long-gauge fiber optic sensors, which measure a wide range of parameters, such as strain distribution along the main span, average strains, average curvature, dynamic strains, dynamic deformed shape, vertical mode shapes and dynamic damping [2, 31]. Figure 2-7 presents some of the different sensors and data acquisition systems (DAQ) that were installed in the I-35W Bridge [31]. This bridge can be considered one of the first "smart" bridges to be built in the USA.

Figure 2-7: Sensors installed in the I-35W Bridge.

The previous mentioned failures also drove authorities to implement monitoring systems in important bridges throughout the country. One of the many examples is the Manhattan Bridge that crosses the East River in New York City. In 2007 this bridge was installed with a SHM system composed of two optical inclinometers, two optical extensometers, a temperature sensor, a monitoring station, SOFO sensors of 6 meters on one main cable and two Bragg grating strain sensors compensated in temperature placed at the anchors on individual strands [32]. Another example is the Huey P. Long Bridge over the Mississippi River, in New Orleans. In this case, the bridge was embedded with a monitoring system composed of an array of 777 vibrating wire strain gauges and 50 electrical resistance strain gauges intended to quantify axial and bending load effects on the truss structure, as well as several tiltmeters and temperature sensors [2, 33].

In China, sophisticated SHM systems have been implemented in bridges, buildings, tunnels and high-speed railways. Some of the infrastructures incorporated with health monitoring systems are the Xihoumen Bridge and the Nanjing 3rd Bridge. The Xihoumen Bridge, located in Eastern China, is currently China's longest suspension bridge with a main span of 1650m. The SHM system implemented into this bridge consists of seven temperature and humidity integrated sensors, seven displacement transducers, ten anemoscopes, 14 Global Positioning System (GPS) devices, 16 inclinators, 24 accelerometers, 46 temperature sensors, 123 wind pressure sensors and weigh-in-motion sensors placed in each lane. The Nanjing 3rd Bridge is a cable-stayed bridge with a main span of approximately 650m that crosses over the Yangzi River. This bridge has an operational SHM system that regularly monitors vehicle loads, wind, temperature, tension in stay cables, deformation and vibration of the deck. This system was put to the test during the earthquake of March 11, 2011, which, after measured, indicated that the stress of the deck or tension in the cable was not that different from any given day, implying that the bridge did not suffer any damage during the earthquake.

In Portugal, there are also some bridges with integrated SHM systems, such as the Vasco de Gama Bridge and the Lezíria Bridge. The Vasco da Gama Bridge was built in 1998 and connects Montijo to Lisbon over the Rio Tejo in Lisbon, Portugal (Figure 2-8) [34]. Being an important infrastructure in the access to the city of Lisbon, the Vasco da Gama Bridge was incorporated with a monitoring program composed of electrical sensors for measurement of joint movements, temperature variations, wind velocity and direction, strains, and accelerations. The monitoring system continuously collects new measurements and compares them to a zero state condition which corresponds to the initial measurements performed after the bridge was constructed. There were also set up several warning levels, which correspond to the different

levels of intervention that may be needed, e.g., closing the bridge to traffic, conducting visual inspections, or developing particular retrofit actions. Curious to know that until now no threshold has been attained demanding unexpected correction measures [34].

Figure 2-8: Ponte Vasco da Gama, Lisbon, Portugal.

The Lezíria Bridge, in Carregado, is also an example with a SHM application. This monitoring system was the result of a joint development between the Portuguese company BRISA Auto-estradas de Portugal S.A. and the Faculty of Engineering of the University of Porto. Accelerometers were installed in critical sections of the superstructure, and in the foundations at different depths, in order to characterize the seismic action on the structure. This monitoring system is also composed of interconnected optical and electrical sensors distributed along the bridge and a central observation post, connected through a network of fiber optic cables. To prevent another disaster such as the Hintze Ribeiro Bridge, sonars were also incorporated to monitor the streambed around the two piers [35].

Other examples of bridge SHM systems in Portugal are the overpasses of Metro do Porto railway system and the Bridge over Rio Sorraia in Santarém owned by BRISA Auto-estradas de Portugal S.A..

2.5. Summary and Conclusions

Even though tragic, each of the failure cases reviewed in this chapter has given its unique contribution to the general knowledge of bridge construction, inspection, and maintenance. The Tacoma Narrows Bridge failure alerted engineers to the dangers of resonance; the Silver Bridge failure focused attention on the lack of maintenance and material corrosion issues. The Schoharie Creek Bridge and the Hintze Ribeiro Bridge failures highlighted the dangers of bridge scour, and finally, the I-35W Bridge and Seongsu Bridge failures underlined

the importance of the construction stage, so that problems are not built-in into the bridge. The investigation of each of these failures and the knowledge gained from understanding the conditions on which they occurred help engineers to find ways to ensure that similar failures can be prevented in the future.

Furthermore, the current practice of visual inspections has been identified as a shortcoming in bridge condition assessment, which gives indications that the BMSs should be upgraded with some more quantitative information regarding the structural condition of the bridges. A review of bridge events performed by McLinn [36] also strongly suggests that inspections may need to be improved, and that inspection alone is not sufficient to guarantee bridge reliability, because it does not include all time-dependent failure modes and causes. Therefore, improvements in damage detection and quantitative measures are needed to optimize BMS [30]. It is the author's belief that any proposal for bridge safety and maintenance should be based on results from long-term monitoring as well as visual inspections along with NDT. This approach will contribute to a much more reliable condition assessment and, therefore, engineers and/or owners will be provided with more quantitative information to support their decisions.

Currently, there are several companies with the single purpose of developing and implementing SHM technology, such as SMARTEC S.A., in Switzerland. SMARTEC was founded in 1996 and it is currently part of the Roctest Group, a manufacturer of instrumentation for civil engineering, geotechnical, and industrial applications. This company has already developed more than 500 monitoring projects worldwide, including the I-35W and the Manhattan Bridges. Several national and international associations have also been founded regarding safety and maintenance of bridges. Some examples are the Portuguese association ASCP (Associação Portuguesa para a Segurança e Conservação de Pontes) which represents Portugal in the international association IABMAS (International Association for Bridge Maintenance and Safety).

3. STRUCTURAL HEALTH MONITORING PROCESS

3.1. Introduction

SHM of bridges is a research field that became known in the late 1980s. The term "health", which is familiar to us in terms of medicine, is herein applied for structural engineering, implying that the same principals applied by medicine in regard of the human body are also applied by engineers regarding infrastructures. When a person is unhealthy, the nervous system detects an anomaly and it transmits the information to the brain. The person addresses a doctor in order to prevent further growth of the illness and, after undergoing detailed examinations, the doctor establishes a diagnosis and proposes a cure. The same principle can be applied to civil infrastructures. The main goal of SHM is to, just like the human nervous system, detect unusual behaviors within the structure. When this happens, the condition is detected and a detailed inspection (examination) takes place in order to find a diagnosis and to repair the anomaly. A comparison between the two processes is presented in Figure 3-1 [37, 38].

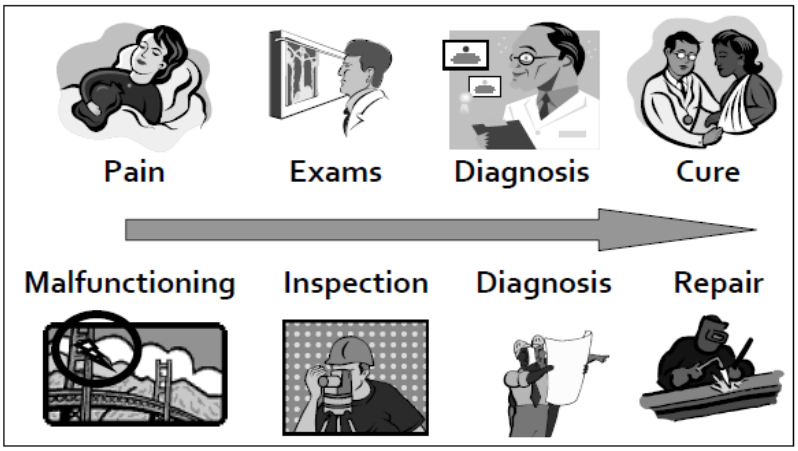

Figure 3-1: Comparison between human body and civil infrastructures.

SHM is currently defined as the process of implementing a damage detection strategy for engineering infrastructures that aims to provide, at any moment during the life of a structure, a diagnosis of its current state. This purpose can only be achieved by observing the system over time and by periodically extracting its dynamic response from an array of sensors, which is used to extract damage-sensitive features and create statistical models upon them. By carrying out this process continuously during the service-life of a structure, SHM systems can provide periodical information regarding the ability of the structure to perform its function, by taking into account the aging and the degradation of the structure as a result of operational and environmental conditions. SHM systems have also the potential to be helpful after extreme

events, such as earthquakes, where quick checks can be performed, providing the user, in near real time, with trustworthy information about the integrity of the structure [39].

3.2. Economic and Safety Considerations

The main purpose of SHM is promote safety and ultimately to prevent catastrophic failures. However, associated with the life safety benefits of this technology, there are also strong economic factors. SHM systems are, after all, an investment and, as any investment, they must prove their effectiveness not only in improving bridge safety but also in reducing the overall life-cycle-cost of bridges. Well-designed and integrated SHM system can prove to be cost effective for both newly built structures and for existing ones. The benefits of installing a SHM system on a bridge depend on the specific application. Nevertheless, there are general benefits common to all applications, such as [31]:

i) Reducing uncertainty: when making decisions regarding the structure, bridge owners always have to consider the worst case scenario as information about the actual condition of the materials, the real load actions or even the structure aging are unknown factors; SHM systems help to reduce such uncertainties allowing the owner to make well-informed decisions based on quantitative data; monitoring systems can also help decreasing insurance costs by reducing the uncertainty associated with the insured risk;

ii) Discovering damage in time: very often damage or deficiencies occur in such a way that cannot be identified by standard inspections; appropriate SHM systems can provide real time information about these issues making it possible to take appropriate actions in advance; early detection of a structural malfunction allows prompt intervention with lower maintenance costs; well-maintained structures have an improved durability, which decreases the direct economic losses (repair, maintenance, reconstruction) and helps to increase the safety of the structure and of its users;

iii) Discovering unknown structural reserves: SHM systems have the potential to uncover structural reserves that were not taken into account during the designing process, allowing a better exploitation of the materials and an increasing in the safety margins and lifetime of the structure without any intervention being needed;

iv) Allowing structural management: current system maintenance is usually done in a time-based mode; SHM technology, being a sensing system that monitors the structure's response and notifies the operator that damage has been detected, can optimize those systems by turning them into condition-based maintenance;

maintenance, repair or replacements will only the executed if necessary, resulting in a decrease of the total maintenance costs;

v) Monitoring increases knowledge: learning how materials and structures perform in real conditions can improve the designing process for future structures, leading to cheaper and safer structures with increased reliability and performance; often making a small investment at the start of a project can bring about savings later in the project by optimizing the design and uncovering weaknesses in time.

For new bridges, the initial investment of a SHM system can vary between 0.5 % and 3% of the total bridge construction cost. This cost includes the hardware, the installation and the configuration of the monitoring system. In addition, every year the management of the monitoring system plus the data analysis usually adds 5% to 20% of the SHM system cost. As a result, over the first ten years of an average-size bridge, having a SHM system installed will require and investment between 2% and 5% of the total construction cost [2, 31].

Assuming that a percentage of newly constructed bridges possess some type of construction defect and that the repair and the indirect costs associated increase considerably alongside the lifetime of the bridge, it is highly beneficial to have a SHM system that detects these errors early, when they are easier and cheaper to correct or preferentially when the bridge is still within the warranty period, typically two to five years. During construction, SHM systems can also be useful to detect and immediately correct mistakes such as non-working bearings, lack of post-tension or wrong thickness of load-bearing elements and defects to water barriers. Observing the bridge behavior during the first ten years can also provide an excellent baseline to compare and assess its future performance or reduction thereof.

Old bridges are often classified as deficient and are repaired or replaced without a quantitative evaluation of their actual condition and load-bearing capacity. Although it is an acceptable procedure from a safety point of view, it is inefficient from an economic perspective. SHM systems can bring some balance to this equation favoring the interest of both safety and economic viewpoints. Supposing that an SHM system is installed on any bridge that is scheduled for replacement, the cost of the SHM system plus data analysis would typically cost 3% of the rebuild cost[1], with the potential to indicate if the bridge needs to be replaced, if it can

[1] As it was mentioned before, the initial investment of a SHM system can vary between 0.5 % and 3% of the total bridge construction cost. Therefore, the cost of implementing a SHM system in a bridge that is going to be rebuilt is the also between 0.5% and 3% of the rebuild cost.

be simply repaired or if it can continuously operate without any type of repair. Assuming that not every bridge needs to be replaced or repaired, and that the costs of the bridges that only need to be repaired are far less than the cost of replacement, economically speaking, the end result would always favor the installment of an SHM system [31].

It is important note that while SHM systems are a mechanism of warning of failure, thus enhancing safety. However, they are not a black box and so they cannot alone ensure a higher level of safety, or even a better method of maintenance. SHM systems alone cannot ensure a decrease in the level of maintenance or even an increase in the periods between maintenance. If properly designed, however, they can reduce the amount of unnecessary inspections and ensure that degradation is tracked, providing the owner with consistent and updated estimates of deterioration (quantity and general location), capacity, and remaining service life.

3.3. Statistical Pattern Recognition Paradigm

There are various ways by which the discussion of SHM can be organized. Herein, the SHM process is broken down into the four-stage SPR paradigm as illustrated in Figure 3-2 [2]. This process includes: (i) Operational Evaluation (ii) Data acquisition (iii) Feature Extraction (iv) Statistical Modeling for Feature Classification.

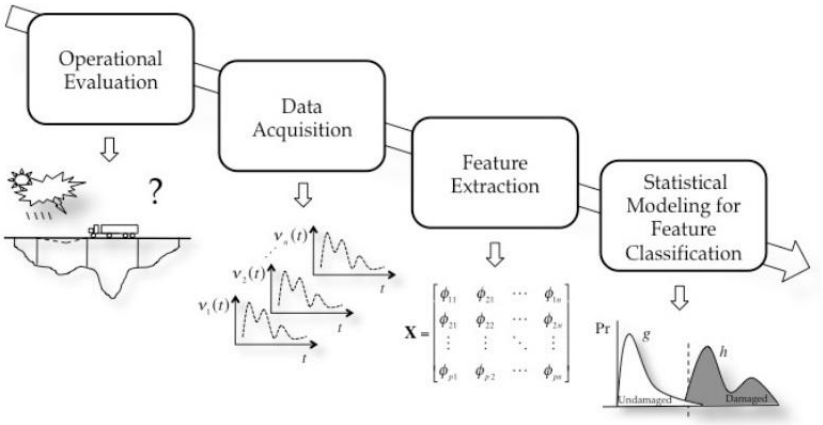

Figure 3-2: SPR paradigm.

3.3.1. Operation Evaluation Stage

Operational evaluation attempts to set up a global view of the whole SHM process by establishing the benefits of implementing a SHM system, defining the damage that needs to be detected and setting limitations on what will be monitored and how the monitoring will be

performed. For the most part, this process attempts to answer four questions concerning the implementation of a SHM system:

i) What are the life-safety and/or economic justification for performing SHM?
ii) How is damage defined for the system being monitored and, in case of multiple damage possibilities, which are of the most critical cases?
iii) What are the operational and environmental conditions under which the system to be monitored will function?
iv) What are the limitations on acquiring data in the operational environment?

3.3.1.1. Economic and/or Life-Safety Issues

Economic and life-safety issues are the main driving forces behind the implementation and development of SHM technology. Nowadays every industry wants to detect damage in their infrastructures in the earliest stage possible. For such a thing to happen, it is necessary for these industries to implement some form of SHM. This technology offers a potential life-safety and economic impact, nevertheless, the economic viability of its implementation should be taken into account. For example, when considering the implementation of SHM technology on a bridge, some questions need to be raised, such as: are the direct costs of carrying out preventative inspections, plus the indirect costs associated with interrupted service, high enough so that implementing a SHM system would prove to be a more viable solution? Is it possible to perform a thorough inspection when some parts are inaccessible without dismantling the bridge? In most cases, on long-term, SHM technology offers a more economical approach, as well as enhanced safety for users [1].

Many of the infrastructures used today are either approaching or exceeding their initial service-life. However, due to economic issues these infrastructures are still being used regardless of their aging. The FHWA estimates that up to 35% of the bridges currently being used in the USA are either functionally or structurally deficient. Furthermore, the repairing cost of these structures can reach a billion dollars. This cost could be drastically reduced by effective SHM methods. Furthermore, in the future, SHM could provide the technology to evaluate the structural condition of the bridges after extreme events, such as earthquakes, by determining if bridges are or not safe for operation [1, 40].

It is important to keep in mind that the life-safety and economic benefits brought by SHM technology can only be accomplished if the monitoring system provides sufficient warning so that counteractive actions can be taken before the damage evolves to a failure level.

3.3.1.2. Definition of Damage

There are many ways by which damage can be defined. The most common one among SHM researchers is to define damage as changes to the material and/or geometric properties of a system, including changes to the boundary conditions and system connectivity. The existence of damage does not imply the total loss of system functionality, but rather that the current or future performance of the system has been compromised and it no longer operates in its optimal manner. Normally, damage progressively attains higher proportions until it reaches a point commonly known as failure. At this point, the damage is so severe that it affects the system operation, making it no longer acceptable to the user. Note that in this definition, the collapse is the extreme situation of failure. Damage can be induced to a system under various means, namely, it can accumulate over long periods of time such as in fatigue or corrosion damage, it can be a result of scheduled events, e.g. vibrations caused by subways, or even unscheduled events such as vehicle impacts or earthquakes. Implicit in the definition of damage is the concept that damage is meaningless without a comparison between two different states of a system. Therefore, it is essential to have data regarding the initial state of the system so that the existence of damage can be verified [1].

There have been several examples of damage detection in structures using finite element models, test bed structures in laboratory environment [4] and real-world test bed structures [3]. Some authors choose to intentionally introduce damage into a structure in the attempt to simulate damage without having to wait for it to occur. Other authors simply postulate a damage-sensitive feature and then create an experiment in an effort to demonstrate the effectiveness of this feature. In these particular cases there is no need to define damage. Nearly all laboratory investigations fall into this class [40]. However, when a SHM system is deployed into the field, it is essential that the damage, or damage scenarios, are clearly defined, because it permits to optimize the sensing capabilities and to increase the likelihood of damage detection with sufficient warning.

3.3.1.3. Environmental and/or Operational Constraints

Environmental and operational effects also have an influence on the measured dynamics response of a structure [41]. These variations can sometimes hide little changes in the system's vibration signal that are actually caused by damage. Since damage detection is based on the premise that damage in the structure will cause changes in the materials hereby causing changes in measured vibration data, it is essential to consider the effects of changing environmental and operational conditions. Operational conditions include ambient loading conditions, mass loading

and operational speed while environmental conditions include temperature, wind, and humidity, rainfall and snow.

The effects of temperature variability such as thermal expansion can not only produce changes in the material stiffness but can also alter the boundary conditions of a system. If the structure is unable to expand or contract, the stress arising from it can produce similar or even greater changes in resonant frequencies than damage. Variations in the structure's surroundings or boundary conditions can often produce more significant changes in dynamic responses than damage. In his research, Alampalli [42] reported that, for a 6.76 by 5.26 m bridge span, the natural frequency variations due to the freezing of the bridge supports were far greater than the variations caused by an artificial cut across the bottom flanges of both girders. For completeness, several other situations have been described in the references [41].

Operational variations can also cause severe changes in bridge dynamics. While studying the effects introduced by vehicle mass on dynamic characteristics of bridges, Kim et al. [43] concluded that while for middle and long-span bridges the changes were barely noticeable, for short-span bridges, whose mass is comparatively small when compared to traffic mass, changes become quite noticeable. A simple supported plate girder bridge with a mid-span of 46 m, with the mass ratio of heavy traffic to the superstructure of 3.8%, experienced changes in its natural frequencies of up to 5.4%.

Therefore, field deployment of these SHM systems need to be accompanied by robust techniques to take into account these environmental and operational constrains/conditions in order for its practical applications to be accepted.

3.3.1.4. Data Management

Field deployment of SHM has to be accompanied by careful data management considerations. Sensors and data storage systems need to be protected from both environmental conditions and human interference. The latter often is overlooked when implementing a SHM system even though thefts are an important factor that must be taken into account. Depending on the environmental conditions that the system is faced with, the sensors and the DAQ and storage unit may need to be sheltered in an attempt to delay their eventual deterioration and subsequent replacement. There is also the possibility of power failures, in which case either the system needs to be programmed to automatically restart or an alternative source of energy must be installed. The DAQ and storage unit also needs to have sufficient RAM memory and Hard Disk Drive space to accumulate the measured data.

3.3.2. Data Acquisition Stage

The data acquisition stage is composed of three features: data acquisition, data normalization and data cleansing. The data acquisition portion refers all the decisions and challenges regarding data collection, especially to the DAQ system and sensing technology. An important concept regarding data sensing technology is that these systems do not measure damage. Rather, they measure the response of a system to its environmental and operational loading or to inputs from actuators implemented with the sensing system. Depending on the type of damage to be identified and the sensing technology installed, the sensors readings may be more or less related to the actual presence of damage [2].

3.3.2.1. Data Acquisition

The data acquisition portion involves the selection of the excitation methods, the types and quantity of sensors used, the sensors' locations, the selection of the DAQ, storage and transmittal hardware and also the interval at which the data will be collected. These decisions are heavily influenced by economic factors, since the type and number of instruments used as well as the frequency of which the measurements will be taken are directly related to the total cost of the SHM system.

In recent years, wireless monitoring, as opposed to wired monitoring, has emerged as a promising technology that could deeply impact the field of SHM. Wired monitoring systems, as the name suggests, are monitoring systems with instrumentation points wire-connected to the centralized DAQ system through cables (Figure 3-3) [8]. Sensors are distributed at key locations through the structure outputting analog signals to the DAQ system where data is later sampled and digitized in order to be used in signal processing systems. Data collected may be analyzed on-site or may be transferred to a control center where experts or computers perform structural diagnosis and prognosis. The length of the cables connecting the sensors to the centralized storage unit can go up to 300 meters. However, the longer the signal travels, the higher the chances of signal degradation due to noise surrounding the cable. After reaching the centralized DAQ system, the analog signals are put through an analog-to-digital converter that discretizes the analog waveforms so relevant engineering quantities (e.g. modal properties and global displacements) can be derived from the raw digitized data.

The down-side of this system is the installation of all instrumentations. Since data cables require high fidelity, their unit price as well as its installation are quite expensive. In existing structures cables are very difficult to install due to thick walls and floors, consequently sensing systems are only able to provide data from limited locations on a structure. The cost of

installation can go up to 25% of the total cost of the monitoring system and the installation itself can take up 75% of the total testing time for large-scale structures [40]. Another setback of this monitoring system is related to maintenance issues. The constant changes in temperature and humidity, as well as exposure to weather conditions, can quickly deteriorate the cables and sensors, which can compromise the economical viability of the monitoring system.

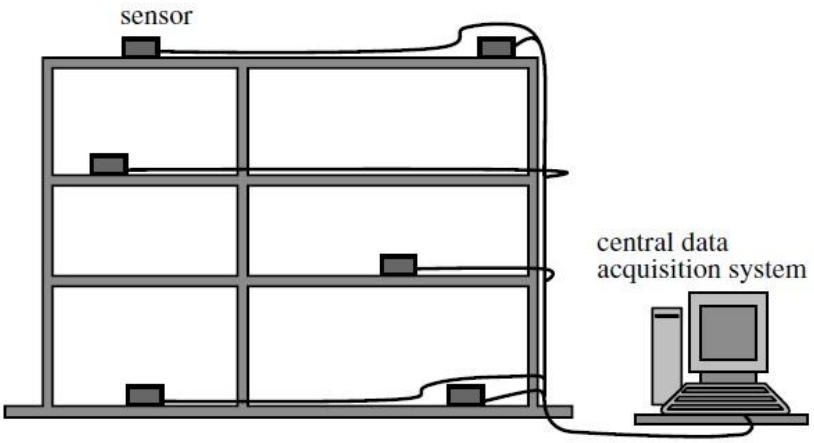

Figure 3-3: Schematic representation of a wired SHM system.

Wireless monitoring arose to overcome the cabling problems of the conventional wired monitoring systems. The use of a wireless transmission eliminates several problems such as extensive cabling, signal deterioration over long transmission distances and damage to instrumentation or computing equipment as a result of the surrounding environment. A schematic representation of a wireless sensor network can be seen in Figure 3-4 [8].

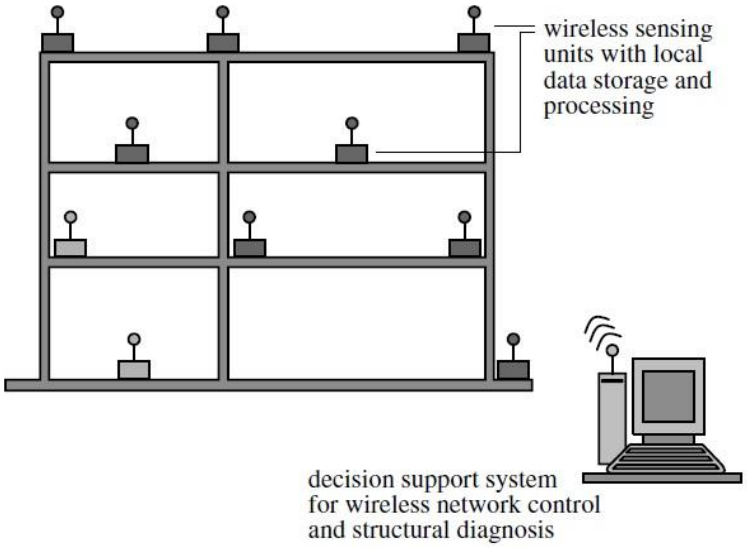

Figure 3-4: Schematics for wireless SHM system.

By overcoming some of the problems regarding wire-monitoring, a higher density network can be established. Each wireless sensing unit can be composed of a microcontroller, a wireless transmitter, DAQ circuitry, actuators and sensors, making it possible for each unit to either individually acquire data and process it locally or communicate with the central processing unit [8, 40]. By doing that, the data acquisition and a part of data processing can be moved toward the sensors, making a clear distinction between this system and the traditional configuration.

Wireless networks also offer a distributed computing environment, which makes it possible to extend analysis capabilities at the sensing nodes allowing multi-tiered diagnostic and prognostic decision making. Therefore, sensing nodes can perform damage diagnosis and prognosis using individual sensors, and then fuse the extracted information with the information provided by the multiple sensors at each node. This information is then combined with the information from other sensing nodes. After the data are collected and fused, a diagnosis takes place and the results are assembled at the system level. In Figure 3-5 is a representation of the multi-tiered decision analysis paradigm [8].

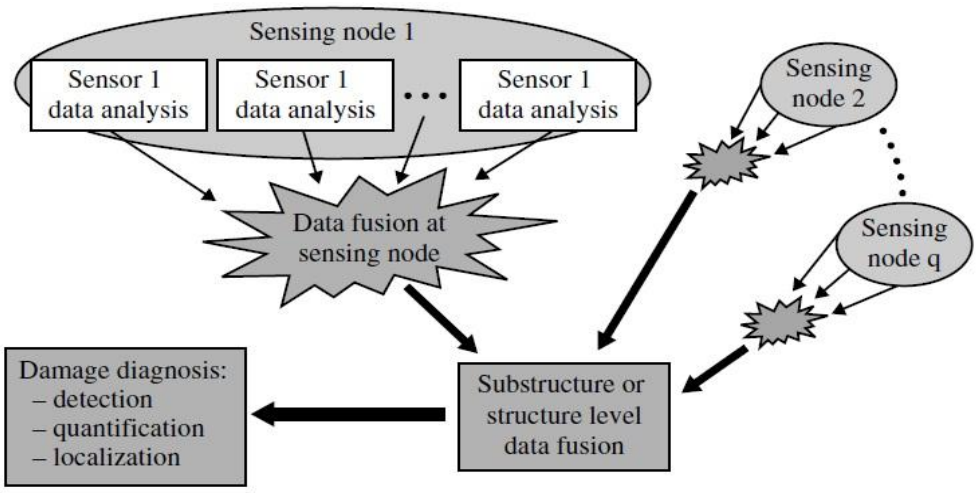

Figure 3-5: Multi-tiered decision analysis paradigm.

Additionally, some of the sensing technology, currently used in data acquisition, will be described.

- Accelerometers

Accelerometers are used to measure accelerations, shocks or vibrations and are the most common type of sensor used in SHM. These devices are very useful in monitoring mainly

because by measuring the accelerations it is possible to determine the angle of the device (which can determine if the structure is tilted) or even the way that the device is moving (which can determine the structure's movement). Accelerometers can be found in many modern devices, like cell phones or digital cameras. In these cases, accelerometers allow screens to change their orientation according to the angle at which the device is held. In the field of engineering there are several types of accelerometers, such as piezoelectric accelerometers and capacitive accelerometers.

Piezoelectric accelerometers are composed of a piezoelectric crystal element and an associated mass that is fixed to a supporting base. The piezoelectric crystal has the ability of emitting a change when subjected to movement. Therefore, when the base moves, the mass compresses the crystal element, which in turn emits a signal. By obeying the second Law of Newton (force is equal to mass times acceleration), the signal's charge is proportional to the applied force, which is proportional to the acceleration. Piezoelectric accelerometers are usually contained inside a protecting box, which shields the sensor from environmental conditions [38, 44]. Figure 3-6 shows a schematic representation of a piezoelectric accelerometer [45].

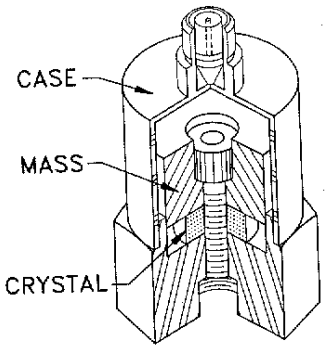

Figure 3-6: Schematics of a piezoelectric accelerometer.

Capacitive accelerometers are able to measure both static and dynamic acceleration forces. This type of accelerometer measures accelerations in a similar way to the piezoelectric. In this case the sensor consists of two plate capacitors, parallel to each other and both charged with an electric current. If a moving mass alters the distance between the metal plates, the electrical capacity of the system will change. By measuring this change it is possible to determine the force in action, which in turn will determine the acceleration (once again resorting to Newton's Second Law of motion) [38, 44].

- Fiber Optic Sensors

In recent years, the use of fiber optic sensors (FOSs) has increased considerably. These sensors are mainly used in SHM applications to measure variations in strain or temperature and they offer distinct advantages when compared to the conventional strain gauges sensors, such as: being able to withstand harsh environmental conditions; since they are non-conductive, these sensors are unaffected by electromagnetic or radio interferences which allows a noise free transmission of data; their small size and weight make the installation of them into any structure; and since they are not affected by corrosion, FOSs are ideal sensing technology for long-term monitoring [44].

Optical fibers are usually made of silica glass with a core region and cladding surrounding the core to guide the light. Additionally there is also a layer of plastic surrounding the silica glass, which prevents it from breaking and adds flexibility to the fiber. Light travels by being reflected continuously between the cladding (Figure 3-7 shows a schematics of this process). Often it is necessary to further coat the cables so they can withstand environmental conditions [44].

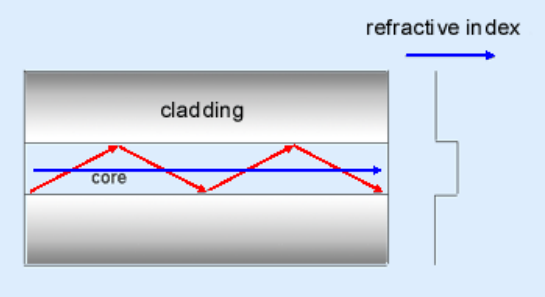

Figure 3-7: Schematic of an optical cable.

The principle behind fiber optic sensing technology is that depending on the condition of the cable, the light patterns of waves transmitted through the optical cable will change. A light beam is first sent through the cable to the sensor. The sensor receives the beam and sends back an optical signal to a measuring device. Finally the measuring device analyses the received information comparing it to the signal that was initially sent. The end result is the measurement that represents the amount of strain on the structure where the sensor is located.

- GPS

The GPS technology has proven to be a great solution in terms of measuring infrastructure deflections. GPS systems use radio waves and GPS satellites to determine the

exact position of the device. Radio signals are broadcasted from GPS satellites with their position and time. A GPS device receives this information and, knowing the exact location of the satellite, determines[2] its own location. Therefore, GPS systems can be used to accurately measure relatively large displacements, such as lateral displacements at the top of tall buildings and bridges towers, and horizontal movements of expansion joints in bridges. Depending on the situation, errors in measurements can be expected, e.g., the presence of particles in the atmosphere can sometimes delay the signal wave causing miscalculations.

- LVDT

The Linear Variable Differential Transducers (LVDTs) are used to measure displacements, which are obtained through induced current variation in a solenoid by displacement of a magnetic core in its interior.

As shown schematically in Figure 3-8, transducers consist of a core, which moves freely along the axis of measurement, and three transformer windings: a primary winding and two secondary windings, one on either side of the primary winding [38, 44, 46].

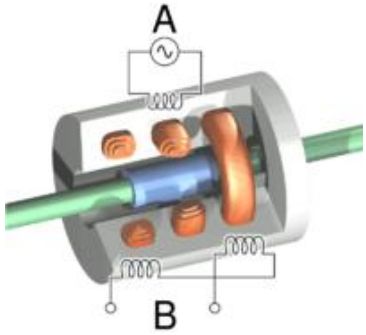

Figure 3-8: Schematics of a LVDT sensor.

The outputs of the secondary windings are wired together so that the voltages induced in each are staggered. When the primary winding is powered with an AC alternating voltage, it generates an inductance current in each of the secondary windings. The core's position determines the magnetic connection between the primary winding and the secondary windings. When the core is at the same distance from both secondary windings, no voltage appears at the secondary outputs (since the voltage induced in both secondary windings are equal). When the

[2] Based on the fact that radio waves approximately travel at the speed of light, the GPS determines the time it took for the signal to get from the satellite to the device. For precision purposes usually this operation isn't limited to only one satellite. The receiver calculates the distances for a number of satellites and verifies if they all converge in one point.

core moves, the inductances in the secondary windings change. The magnitude of the output voltage has a linear correlation with the position of the core. Figure 3-9 shows an actual LVDT [38, 44, 47].

Figure 3-9: LVDT sensor.

- Strain Gauges

Strain gauges work based on the principle that the resistance of an electric conductor varies with the force applied to it. When the strain gauge is stretched, its resistance increases and when it is compressed its resistance decreases. The changes in resistance are always proportional to the deformations. Due to its characteristics, strain gauges are usually attached to the surface of the structural components being monitored [44].

Ideally changes in resistance should only happen due to superficial deformations of the material the sensor is glued to. However, in real-world applications, misleading readings can occur as a result of the glue that connects the gauge to the material and due to temperature variability.

- Tiltmeters

This sensor is used to measure slight changes in the inclination of a structure or its members. Generally, it can measure inclinations in either one direction (uniaxial) or two directions (biaxial), depending on the application [38]. Tiltmeters can improve safety both in the construction stage and the service-life of a structure. During construction it can be used to monitor structural or foundation movements and alert engineers if the allowed limits are being exceeded. During the service-life they can be used to closely monitor the structure's movement. In many applications, especially on bridge decks, the tiltmeters can be used to estimate curvatures.

3.3.2.2. Data Normalization

The normalization of the data measured under varying conditions is vital to the damage identification process. For example, the measurements taken from the Alamosa Canyon Bridge in New Mexico showed that the fundamental frequency of the bridge had a 5% variation during a 24-hour test period. This variation was caused by a large temperature gradient between the east and west sides of the bridge deck during the day [40]. If that variability is not remove from the data, it can be taken as a false-positive indication of damage.

Therefore, data normalization is a procedure of separating the changes in sensor readings, so that signal changes caused by operational and environmental variations can be separated from structural changes caused by actual damage. One of the most frequent procedures is to normalize the measured responses (outputs) by measured inputs. When there are a lot of changes regarding the environmental or operational conditions, a common practice is to normalize the data in a temporal fashion in order to make easier the comparison between data measured at similar times of an environmental or operational cycle. Figure 3-10 and Figure 3-11 illustrate situations where measures of operational or environmental parameters need or do not need to be included into the normalization procedure [48]. In Figure 3-10 damage introduces changes in the feature distribution that are similar to those introduced by an environmental variability, which indicates that operational or/and environmental parameters will need to be measured so that they can be incorporated into the normalization process. On the other hand, in Figure 3-11 damage introduces changes in the feature distribution different to those caused by operational or/and environmental effects. In this case, there is no need to establish an environmental parameter [48].

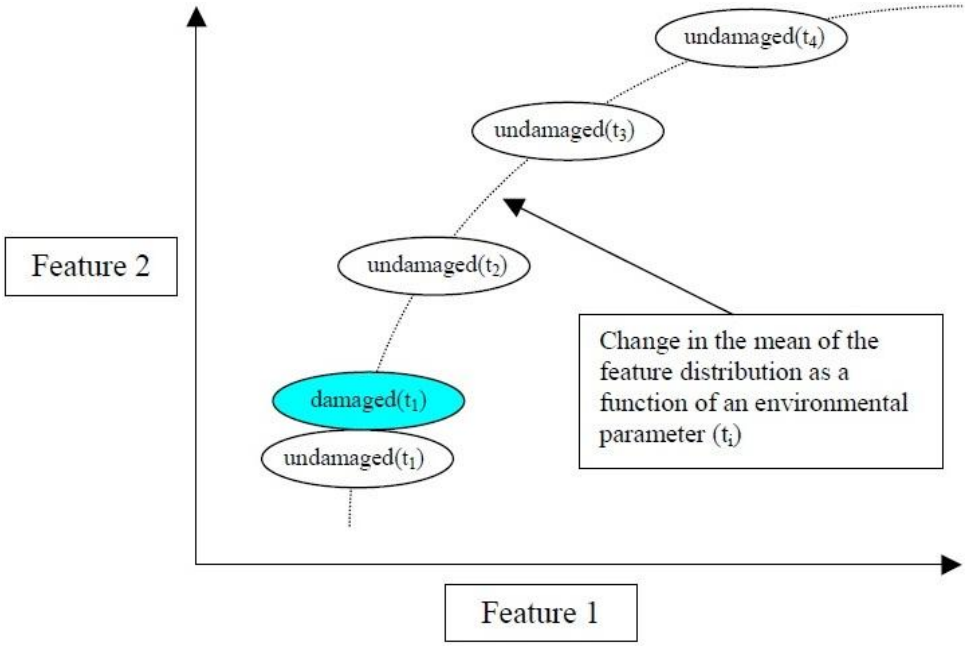

Figure 3-10: Damage introduces changes similar to environmental variability.

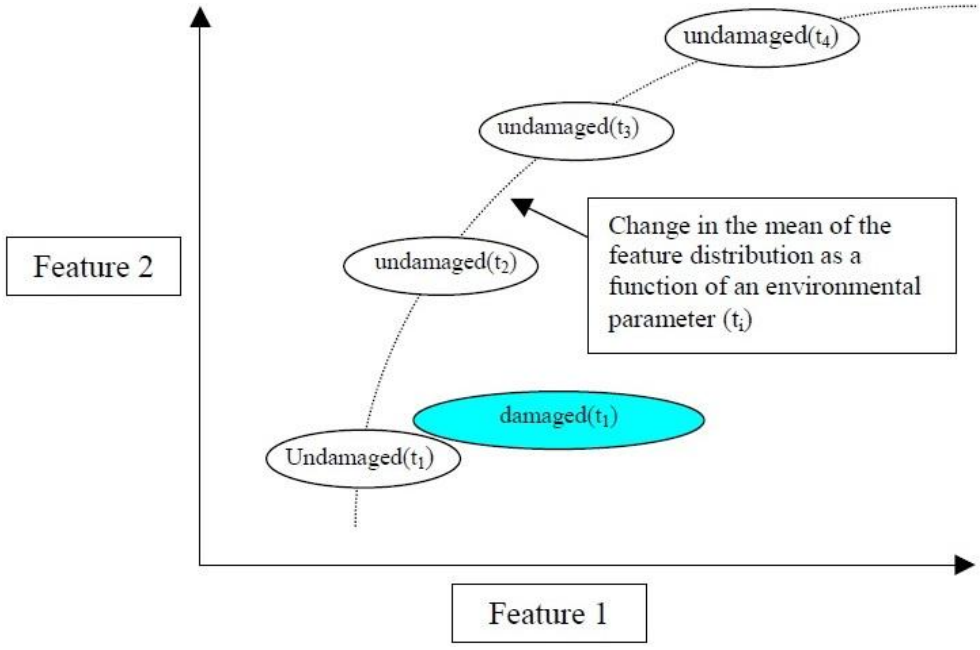

Figure 3-11: Damage introduces changes different from environmental variability.

It is also possible to normalize the data by measuring directly the varying environmental or operational parameters. Identifying and minimizing the causes of these variability's is a crucial step toward a good SHM system, and even though it is practically impossible to eliminate all sources of variability, by making the appropriate measurements it is possible to statistically quantify them. Variability can result from changes in environmental (e.g.

temperature and wind) and test condition, changes in the data reduction process and unit-to-unit inconsistencies [1, 40].

3.3.2.3. Data Cleansing

Data cleansing is the process of detecting and removing the corrupt or inaccurate data from the raw data. This step is generally executed according to the knowledge of those directly involved with the data acquisition process. For instance, an inspection of the test set-up might reveal that a sensor was loose. As a result that set of data or the data from that sensor may be selectively deleted from the feature selection process, depending on the judgment of the persons performing the measurement. Signal processing techniques like re-sampling and filtering can also be considered data cleansing procedures [1, 39].

3.3.3. Feature Extraction Stage

Feature extraction is the area of the SHM process that receives the most attention in terms of technical literature [1]. A feature is a characteristic of the measured response that is extracted via parameter estimation, signal processing, or other signal inspection technique. Ideally, a feature should have characteristics regarding sensitivity, dimensionality and computational requirements. It should be very sensitive to damage and, for the most part, insensitive to everything else, have the lowest dimension possible and also be computable with minimal assumptions and CPU (central processing unit) cycles. Preferably, the best damage-sensitive feature would be the simplest feature possible that could distinguish between the damaged and undamaged system.

The feature extraction process can be defined has the identification of features that allows one to distinguish between the damaged and undamaged system. In most cases, feature extraction procedures inherent a form of data compression (or condensation) and data fusion. The condensation of data is necessary and beneficial, especially in long term monitoring where sets of data needed for comparison become increasingly abundant. Since data can be acquired from a structure over a long period of time and in an operational environment, data-compression techniques must keep sensitivity of the chosen features to the structural changes of interest in the presence of operational and environmental variability.

There are numerous methods that can be employed in order to identify features for damage detection. A basic method for feature selection is based on past experience, especially if damaging events have been formerly observed for that system. Another mean of identifying features is to apply engineered flaws, similar to ones that are expected during actual operating

conditions, to laboratory specimens and develop a preliminary understanding of the parameters that are sensitive to the expected damage. The flawed system can also be used to verify if the diagnostic measurements are sensitive enough to differentiate between features identified from the damaged and undamaged system [1, 2]. The employment of analytical tools like FEM can be a great asset in this process. Appropriate features can also be identified by performing damage accumulation tests where structural components of the system under study are subjected to realistic loading conditions. This process can involve fatigue testing, induced-damage testing, temperature cycling or corrosion growth in order to gather certain types of damage in an accelerated manner. The types of analytical and experimental studies described above can give an insight into the features better suited for a SHM system. Usually the most appropriate feature is a result of information gained from a combination of these sources. This subsection will give a brief overview of some damage-sensitive feature extraction techniques, with special attention being given to AR models and modal parameters.

3.3.3.1. Autoregressive Model

The autoregressive (AR) model is a linear prediction formula that attempts to predict an output of a system based on the previous outputs. For a time series $\mathbf{s} = \lfloor s_1, s_2, ..., s_n \rfloor$, the AR model with p autoregressive parameters, AR (p), can be written as,

$$s_i = \sum_{j=1}^{p} \phi_j \times s_{i-j} + e_i \,, \qquad \textbf{(3.1)}$$

where s_i is the measured signal and e_i is the residual error at the i^{th} signal value. The unknown AR parameters, ϕ_j, can be estimated by using either the least squares or the Yule-Walker equations [49].

In SHM, the AR model can be used as a damage-sensitive feature extractor based on two approaches: (1) using the AR parameters, ϕ_j ; and (2) using the residual errors, e_i. The first approach consists of fitting AR models upon data from the damaged and undamaged structure, and then the AR parameters, ϕ_j, are used directly as damage-sensitive features. The second approach consists of fitting an AR model upon data from the baseline condition, and then it is used to predict the response data obtained from a potentially damaged structure. The residual error, which is the difference between the predicted and measured signal, is calculated at time i using the equation

$$e_i = s_i - \hat{s}_i\,, \tag{3.2}$$

where $\hat{s}_i$ is the predicted i^{th} signal value and s_i the measured value. This approach is based on the theory that the presence of damage will introduce either a linear variation from the baseline condition or nonlinear effects in the signal and, since the linear model was developed based on the data from the baseline condition, it will no longer be able to accurately predict the response of the system once it is damaged. Note that for a fitted AR (p) model, the residual errors can only be computed for $i > p$ time points [2].

The main issue with AR models is generally that the order is an unknown value. A high-order model may be a perfect match for the data, but it will be harder to process and it will consume many CPU cycles. Additionally, a higher order model might not generalize well to other data sets from the same system. On the other hand, a low-order model may not be enough to capture the system's physical response. In order to determine the most appropriate model order, several techniques can be used. In this case, it is used the Akaike's information criterion (AIC) [50]. The AIC provides a mean for model selection and can be written as

$$AIC = n\log\left(\frac{RSS}{n}\right) + 2p\,, \tag{3.3}$$

where n is the number of data points, RSS is the residual sum of squares and p is the number of parameters in the model. The RSS is a measure of discrepancy between the data and the estimation model. The RSS can be written as

$$RSS = \sum_{i=1}^{n} e_i^2\,. \tag{3.4}$$

The AIC assumes a tradeoff between the fit of the model and the model's complexity. The first term of the Equation (3.3) is related to how well the model fits the data, i.e., if the model is too simple its predictions will not be accurate and the residual errors increase. On the other hand, the second term is a penalty factor related to the complexity of the model, which increases with the number parameters used in the model. The AIC methodology attempts to find the model that best explains the data with the minimum parameters, therefore the ideal model is the one with the minimum AIC value.

3.3.3.2. Modal Properties

In bridge monitoring, dynamic or vibration analysis is a subset of structural analysis that is concerned with the behavior of structures under dynamic loading, such as traffic, people, wind, and earthquakes. Dynamic analysis can be carried out to perform modal analysis and to obtain dynamic displacement time series records.

Modal analysis techniques have been widely used in bridge monitoring. Modes are natural properties of a structure, and are determined by its material properties such as mass, damping, and stiffness and by its boundary conditions. Each mode is defined by its modal properties: natural frequency, mode shape, and damping ratio. When boundary conditions or material properties of a structure are altered, its modes will also suffer alterations. For example, if mass is removed from a structure, it will have a different vibration response.

Due to their nature and how they react to changes undergone by the structure, natural frequencies, modes shapes or other properties derived from modes are commonly used as features for damage detection.

3.3.4. Statistical Modeling for Feature Classification Stage

Development of statistical models is the portion of the SHM process that has received the least attention in terms of technical literature. This final stage in the SHM process attempts to implement algorithms that analyze the distribution of the extracted features in order to determine if the structure is damaged. The algorithms used in statistical model development typically fall into three categories: (i) Group classification, (ii) Regression analysis, and (iii) Outlier detection. Both group classification and regression analysis are supervised learning algorithms while outlier detection is an unsupervised learning algorithm. Supervised learning is the given classification of algorithms that are applied when data are available from both the undamaged and damaged structures. On the other hand, unsupervised learning refers to algorithms that are applied when there are only data from the undamaged structure [1, 2].

Group classification attempts to, in a statistically quantifiable approach, discriminate features into “damaged” or “undamaged” categories. By using the experience from prior damaged and undamaged systems and the feature changes associated with previously observed damaged cases, it is possible to deduce the presence, type, and level of damage.

Regression analysis is the process of correlating data features with locations or extents of damage. Rather than being categorized as “damaged” or “undamaged” like in group classification, in regression analysis features are mapped to a continuous parameter, e.g., a

remaining-useful-life temporal parameter. This analysis requires the availability of features from both the undamaged structure and the structure at different damage levels [51].

Outlier detection attempts to answer the following question: when data from a damaged structure are unavailable for comparison, do the observed features point out a significant change from the previously observed features that cannot be explained by extrapolation of the feature distribution? This type of analysis is mainly based on multivariate probability density function (PDF) estimation. The main problem when performing an outlier analysis is that as the dimension of feature vectors increases, large amounts of data are needed to define the density function [51]. Actually, this category has been preferentially used in the civil engineering sector due to the scale of civil structures, i.e. it is not feasible to introduce damage into the structure in order to collect data from the undamaged and damaged structure.

The damage identification in a system can be described in a hierarchical structure (Figure 3-12) that attempts to answer the following questions [2]:

i) Is there damage in the system? (Existence)
ii) Where is the damage in the system? (Location)
iii) What kind of damage is present? (Type)
iv) How severe is the damage? (Extent)
v) How much useful life remains? (Prognosis)

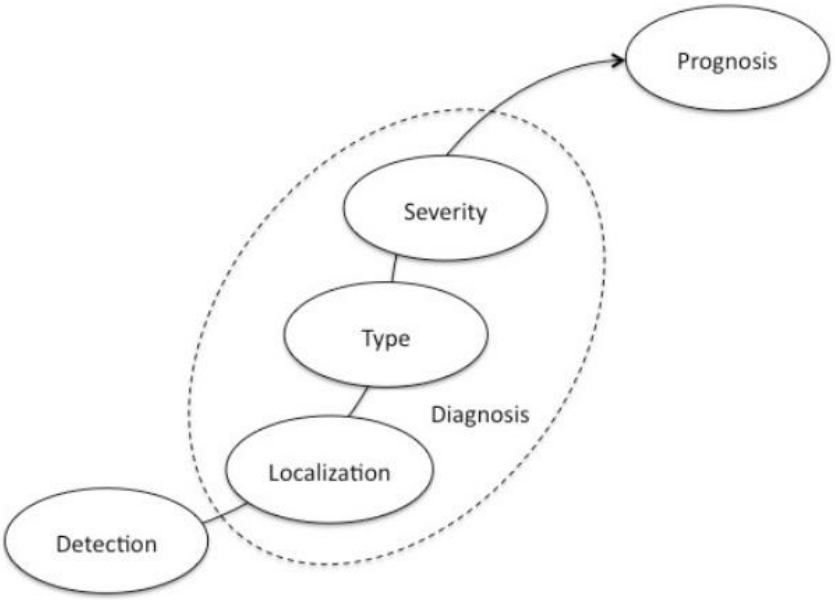

Figure 3-12: Hierarchical structure of damage identification.

Answers to these questions can only be made in the same specific order as the questions are presented, e.g., knowing the location of the damage can only be answered after knowing about its existence. Statistical models are used to answer these questions in definite and quantifiable manner and, by doing so, they will provide knowledge about the damage state of the system. When applied in an unsupervised learning mode, statistical models are generally used to answer the first two questions, regarding the existence and location of damage. In order to identify the type of damage, data from structures with the specific types of damage would be needed so a correlation with the measured features could be made. When applied in a supervised learning mode and joined with analytical models, the statistical procedures can be used to determine the type and extent of damage and remaining useful life of the structure [1, 2].

Statistical models can also be used to minimize false indications of damage. False indications of damage fall into two categories: (i) false-positive (the monitoring system indicates damage when there is none) and (ii) false-negative (the monitoring system gives no indication of damage when damage is present). Although the second category is at first glance the most negative to the damage detection process, since safety issues are at stake, false-positive readings also erode confidence in the damage detection process, as it causes unnecessary downtime and consequent loss of revenue. During the operation evaluation stage it can de decided to allow pattern recognition algorithms to weigh one type of error above the other.

3.3.4.1. Outlier Detection based on the Mahalanobis Squared Distance

The Mahalanobis distance, proposed by Mahalanobis in 1936, is a distance measure used to determine the similarities between sample sets. This procedure is commonly used in cluster analysis and classification techniques. It diverges from the traditional Euclidean distance because it takes into account the correlation between the variables and it is scale-invariant (does not depend on the observations scale). Considering a data set with a mean vector $\boldsymbol{\mu}$ and covariance matrix, $\boldsymbol{\Sigma}$, the Mahalanobis distance between that data set and a new one $\mathbf{x}$ is defined as

$$D = \sqrt{(\mathbf{x}-\boldsymbol{\mu})^T \Sigma^{-1} (\mathbf{x}-\boldsymbol{\mu})}. \quad \textbf{(3.5)}$$

In the context of SHM for feature classification under operational and environmental variability, the mean vector, $\boldsymbol{\mu}$, and the covariance matrix, $\boldsymbol{\Sigma}$, represent the baseline condition (i.e. all state conditions available when the structure is thought to be undamaged) and $\mathbf{x}$ represents a potential damaged state condition. Herein, the author uses the Mahalanobis squared

distance (MSD), or also designated as damage indicator (DI), as a distance measure for multivariate statistics' outlier detection. In these cases, the equation above should be written as follows:

$$DI(\mathbf{z}) = (\mathbf{z} - \boldsymbol{\mu})^T \boldsymbol{\Sigma}^{-1} (\mathbf{z} - \boldsymbol{\mu}), \tag{3.6}$$

where $\mathbf{z}$ is the potential outlier vector belonging to the test matrix $\mathbf{Z} = [\mathbf{z}_1, \mathbf{z}_2, ..., \mathbf{z}_T]$ and the mean vector, $\boldsymbol{\mu}$, and covariance matrix, $\boldsymbol{\Sigma}$, are estimated from the training matrix $\mathbf{X} = [\mathbf{x}_1, \mathbf{x}_2, ..., \mathbf{x}_M]$ [52]. If the feature vector $\mathbf{z}$ has been extracted from the same multivariate normal distribution as the training matrix $\mathbf{X}$, the test statistic $DI(\mathbf{z})$ will be Chi-squared distributed with m DOF,

$$DI \sim \chi^2_m, \tag{3.7}$$

where m is equal to the length of the feature vector. This allows an outlier to be defined as a feature vector with large DI. The assumption of a Chi-squared distribution is key for outlier detection because it allows the definition of a threshold value, c, for a level of significance, α, as follows,

$$c = invF_{\chi^2_m}(1 - \alpha), \tag{3.8}$$

where $invF_{\chi^2_m}$ is the cumulative distribution function of the Chi-squared distribution. As a result, a feature vector is considered to be an outlier when its DI is equal or greater than c [2, 55].

3.3.4.2. Outlier Detection based on Gaussian Mixture Models

The underlying density distribution of the acquired data is very important to the statistical modeling for feature classification stage. The MSD-based algorithm described above is suitable for outlier detection when the training data is multivariate Gaussian distributed. However, it is not possible to ensure that the MSD-based algorithm will work properly in cases where the data are not Gaussian distributed. Therefore, the GMM stands as a useful alternative to overcome those limitations. The GMM is a parametric PDF represented as a weighted sum of multivariate normal density components [53]:

$$p(\mathbf{x} \mid \lambda) = \sum_{k=1}^{K} w_k \times g(\mathbf{x} \mid \boldsymbol{\mu}_k, \boldsymbol{\Sigma}_k) \quad , \tag{3.9}$$

where $\mathbf{x}$ is the feature vector, $w_{k,k=1,\ldots,K}$, are the mixture weights, and $g(\mathbf{x} \mid \boldsymbol{\mu}_k, \boldsymbol{\Sigma}_k)$, are the component Gaussian densities. Each component density is a m-variate Gaussian function given by:

$$g(\mathbf{x} \mid \boldsymbol{\mu}_k, \boldsymbol{\Sigma}_k) = \frac{1}{(2\pi)^{m/2} |\boldsymbol{\Sigma}_k|^{1/2}} \exp\left\{ -\frac{1}{2} (\mathbf{x} - \boldsymbol{\mu}_k)^T \boldsymbol{\Sigma}_k^{-1} (\mathbf{x} - \boldsymbol{\mu}_k) \right\} \tag{3.10}$$

where $\boldsymbol{\mu}_k$ is the mean vector and $\boldsymbol{\Sigma}_k$ the covariance matrix of the k component. The sum of all mixture weights must be equal to unity.

These types of models are frequently used for probability density estimations in a wide range of pattern recognition and machine learning systems. The parameters of the GMM are generally estimated using the Expectation-Maximization (EM) algorithm, an iterative procedure for finding the Maximum Likelihood (ML) estimate in the presence of hidden or missing data. Alternatively, the parameters can be estimated using a Bayesian approach based on a Markov-Chain Monte Carlo method as described in [54]. These parameters can all be represented in the following notation:

$$\lambda_k = \{w_k, \boldsymbol{\mu}_k, \boldsymbol{\Sigma}_k\}, k = 1,\ldots K. \tag{3.11}$$

In the context of the SHM for damage detection, under operational and environmental variability, the GHM is used as follows: (1) determine the number, K, of normal components contained in the training data using the AIC, (2) identify the parameters λ_k of each normal component k (mean vector, covariance matrix, and weight factor), (3) construct a MSD-based algorithm for each normal component k, and finally (4) for each observation, determine the minimum *DI*, i.e. $DI = min(DI_k)_{k=1,..,K}$.

3.4. Shortcomings and Limitations

SHM is based on the principle that the presence of damage will considerably alter the properties of a system (stiffness, mass, and energy dissipation), which in turn will alter the system measured dynamic response [1]. Even though this principle seems to be quite intuitive,

the reality is that its application is not straightforward. The first challenge resides in the fact that damage is usually a local phenomenon and its presence may not even influence the dynamic response of the system in a way that can be perceptible to the sensing system.

Another challenge is the influence of operational and environmental variations when deploying a monitoring system in the field. As already mentioned in Subsection 3.3.1.3, these variations can cause significant changes in the dynamics of a structure, which in turn can mask changes caused by actual damage such as concrete cracking, material deterioration due to aging, or even yielding of steel elements. However, in long-term monitoring, these variations affect not only the structure but also the monitoring system, thus raising the possibility of sensor damage. When sensors are bonded or otherwise placed on surfaces, they may be subjected to extremes of temperatures, large temperature variations (both daily and seasonal), humidity, precipitation, actual immersion (due to possible flash floods which can cause overtopping of bridges), and UV radiation. Therefore, it may be necessary to monitor the sensors themselves. This can be accomplished by either developing appropriate self-validating sensors or by using the sensors to communicate with each other and report their condition. Sensor networks also ought to be "fail-safe", meaning that if a sensor is about to fail, the system should be able to adapt to the new network. Sensor failure does not necessarily mean that a sensor does not work at all, it can also mean that it does not work properly and, therefore, it might transmit false data and, consequently, raising the possibility of false alarms. All these aspects must be carefully considered in order to ensure the long-term reliability of data.

There are also other non-technical challenges that must be addressed before SHM technology can make the transition from a research topic to actual practice. The construction sector is very conservative and the implementation of new technologies needs a clear requirement and motivation in order to be accepted by bridge owners. SHM technology needs to convince owners that it provides an economic benefit over their existing maintenance approaches and regulatory agencies that this technology provides a significant life-safety benefit. Only after the requirements and motivation have been clearly understood, and argued against potential clients, can SHM hope to achieve a breakthrough in its implementation.

Unfortunately, the biggest challenge is that without significant planning and deliberation, most SHM systems end up of being elaborate measures of gathering data, rather than providing means for its efficient management and interpretation. It is vital that the system provides the means not just for recording and displaying responses, but also of analyzing the response so an assessment of the critical aspects of capacity and service-life can be made.

3.5. Summary and Conclusions

The SHM has the potential to improve the BMS. Its potential for economic and life-safety benefits is a strong motivation for this field to evolve and to mature over the years. The SHM main goal is to identify damage in the structure in its early stages. In order to achieve it, some sort of pattern recognition needs to be implemented. Therefore, herein the SHM process is posed in the context of the SPR paradigm. This paradigm can be broken down into four stages: (1) Operational Evaluation, (2) Data Acquisition, (3) Feature Extraction, and (4) Statistical Modeling for Feature Classification. Operation Evaluation attempts to give a global view of the whole SHM process by establishing the benefits of implementing a SHM system, defining the damage that is to be detected, and setting limitations on what will be monitored and how the monitoring will be performed. Data Acquisition defines the type of sensing hardware that is going to be used and which data are going to be selected for the feature extraction process. Additionally, some sort of data normalization and cleansing might be performed for feature enhancement. Feature Extraction is the process of identifying features and performing information condensation. Finally, the Statistical Modeling for Feature Classification attempts to develop statistical models to discriminate damage-sensitive features into, for instance, undamaged and damaged conditions.

Among all the stages of the paradigm, the data acquisition is the one that has showed the most remarkable development in the last years. New smart materials/sensors such as FOS have proven to be a new development with vast potential for the SHM field. The evolution of data transmission technology, such as wireless communication, has also given a tremendous step in creating better monitoring networks. As most civil engineering structures are usually very large, common wired networks are very expensive and hard to implement.

Nevertheless some aspects of this paradigm still need to be improved. One of the main challenges is still to differentiate changes in the structural response caused by damage from changes caused by operational and environmental conditions. For instance, changes in the natural frequencies of a bridge are more likely to be a result of temperature variations than actual damage. It is important to identify all the operational and environmental state conditions so that wrong assumptions are not made regarding the existing of damage and resources are not wasted.

4. APPLICABILITY OF THE SPR PARADIGM: LABORATORY 3-STORY STRUCTURE

4.1. Introduction

This chapter aims to study the applicability of the concepts described in the previous chapter on data sets from a laboratory structure. To that purpose, standard data sets were acquired from a base-excited three-story frame structure, created and tested in a laboratory environment at Los Alamos National Laboratory (LANL) [2]. The data sets are composed of force and acceleration time series measured under various structural state conditions. In order to simulate damage, a bumper mechanism was placed between floors. This mechanism attempts to simulate the fatigue cracks that open and close under operational and environmental loading conditions. The operational and environmental effects were simulated by using different mass and stiffness conditions (non-damage related events). As stated previously in Chapter 3, operational and environmental effects include changes in both the loading conditions and in the material stiffness of the structure. In this case, the changes added to the structure were designed to introduce variability in the fundamental natural frequency up to 7% from the baseline condition, which is a value within the normal range observed in real-world structures [2, 52].

In the context of the hierarchical structure of damage identification, this chapter will be focused on determining the existence and, to the best extent, the location of damage in the structure as an extension to the previous results obtained by Figueiredo et. al [2, 4, 41, 52, 55]. Even thought determining the type and severity are important steps in the damage identification process, robust and reliable damage detection and localization methods must precede those steps, so that the process can be built on solid foundations. To achieve that goal, this chapter will be focused on the application of feature extraction and statistical modeling for feature classification techniques, mainly based on the AR models, the modal parameters, and the Mahalanobis distance.

4.2. Structure Description and Data Acquisition

The three-story building structure (Figure 4-1) consists of aluminum plates and columns assembled using bolted joints which slides on rails only allowing movement in the x-direction. The different leveled plates ($30.5 \times 30.5 \times 2.5$ cm^3) are connected by four aluminum columns ($17.7 \times 2.5 \times 0.6$ cm^3) at each floor, forming a four degree-of-freedom (DOF) system. In addition, a center column ($15.0 \times 2.5 \times 2.5$ cm^3) is attached to the top floor. The purpose of this column is to simulate damage by inducing nonlinear behavior when it makes contact with a

bumper mounted on the floor below (Figure 4-1). The gap between the bumper and the column can be adjusted to vary the extent of impacting that occurs during a particular excitation level. In Figure 4-2 it is possible to see a schematic representation of the test structure [2, 52].

The structure is connected at the base to an electrodynamic shaker, which provides a lateral excitation along the center line of the structure. Both the structure and the shaker are fixed on and aluminum baseplate (76.2 × 30.5 × 2.5 cm^3), and the entire system rests on rigid foam, which minimizes extraneous sources of unmeasured excitation from being introduced through the base of the system. A load cell (Sensor 1) with a nominal sensitivity of 2.2 mV/N was placed at the end of a stinger to measure the input force from the shaker to the structure. Four accelerometers (Sensor 2-5) with nominal sensitivities of 1,000 mV/g were placed at the center line of each floor on the opposite side from the excitation source in order to measure the system's response. Since the accelerometers are located at the center line of each floor they are insensitive to torsion. Additionally, the location of the shaker and the linear bearings minimize the torsional excitation of the system [2, 51].

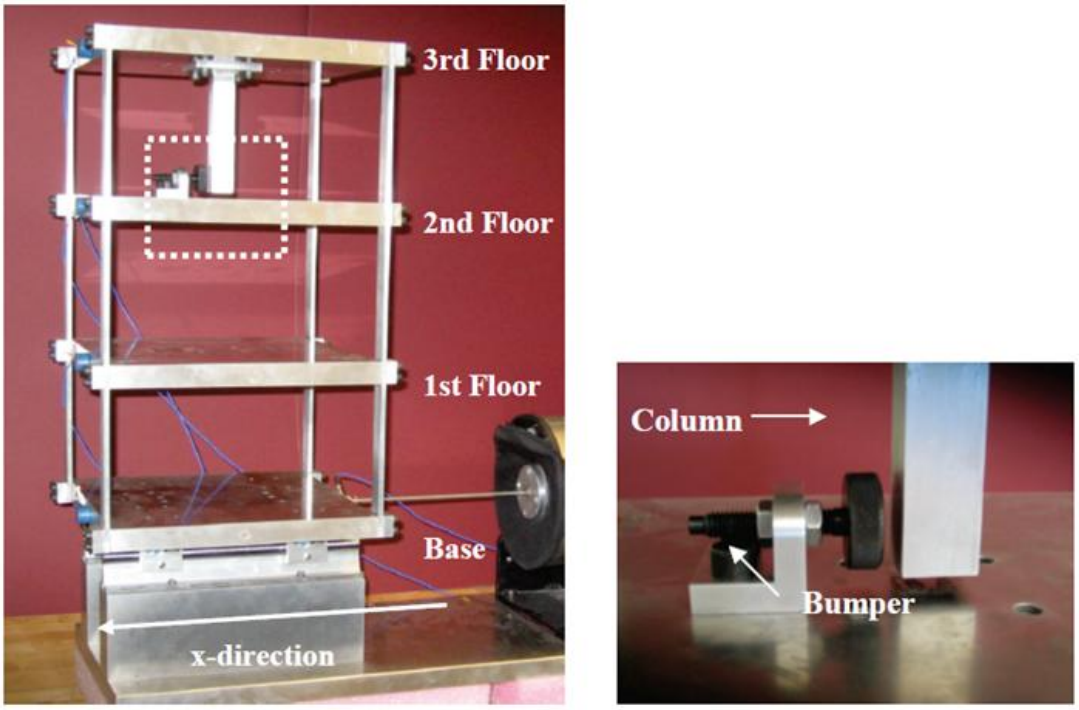

Figure 4-1: Three-story building structure and shaker (on the left); Adjustable bumper and the suspended column (on the right).

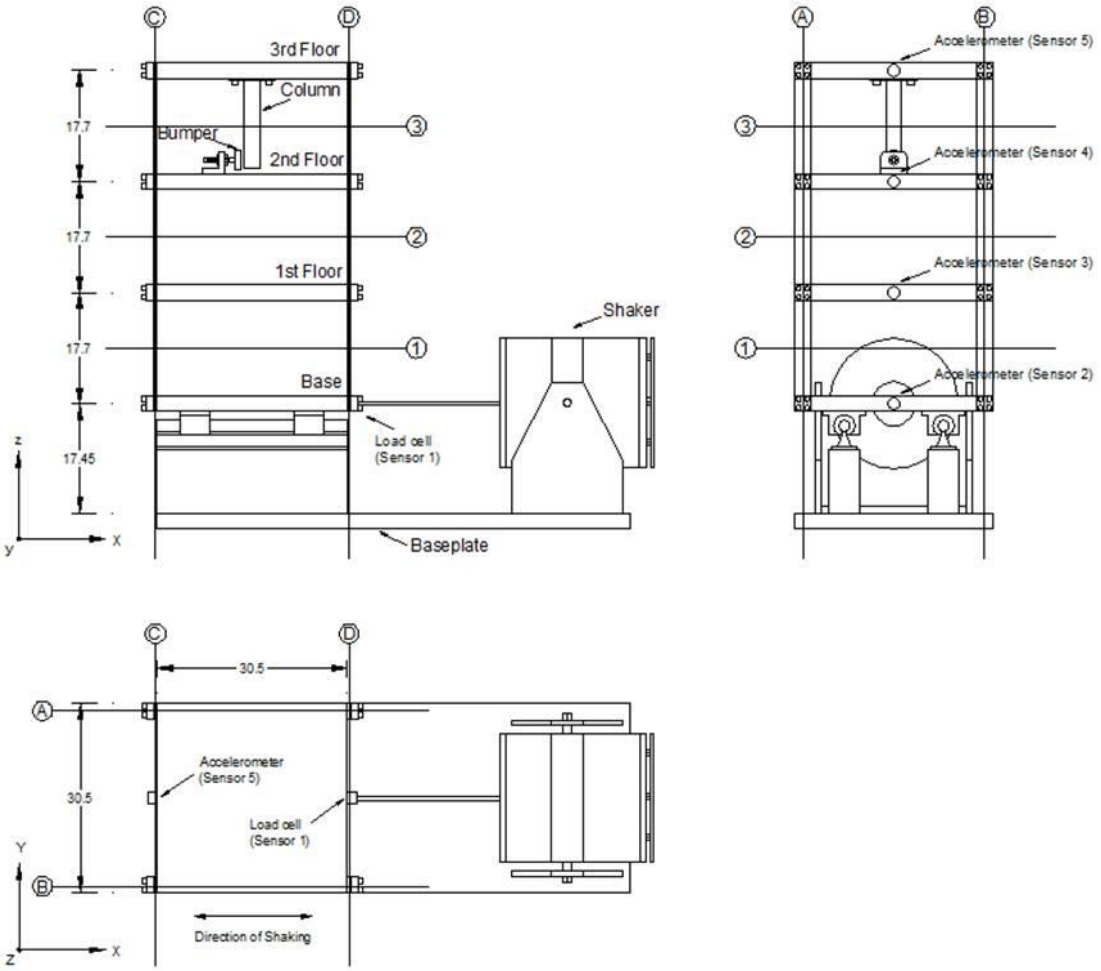

Figure 4-2: Dimensions (in centimeters) of the three-story building structure.

The DAQ system is composed of a Dactron Spectrabook, which was used to collect and process the data. The output channel of this system is connected to a Techron 5530 Power Supply Amplifier that drives the shaker. The location of the five sensors (Sensors 1–5) used in these tests can be found in Figure 4-2. The analog sensor signals were discretized with 8,192 data points sampled at 3.125 ms intervals matching a sampling frequency of 320 Hz. These sampling parameters yield time histories of 25.6 seconds in duration. A band-limited random excitation ranging from 20 to 150 Hz was used to excite the structure. This excitation signal was chosen with the intention of avoiding the rigid body modes of the structure that are often present below 20 Hz. The excitation level was set to 2.6 V RMS in the Dactron system, which corresponds to 20 N RMS measured at Sensor 1.

Force and acceleration time series for various structural state conditions were collected, as shown in Table 1, along with information describing the different states. For example, the state condition labeled “State #6” is described as “87.5% stiffness reduction in column 2BD,” which means that there was a 87.5% stiffness reduction in the column located between the first and second floors at the intersection of plane B and D as defined in Figure 4-2.

The structural state conditions can be classified into four main groups. The first group is the baseline condition, which is the reference structural state (State #1). The bumper and the suspended column are included in the baseline condition, however the space between the bumper and the column ensures that there were no impacts during the excitation. The second group includes the states when the mass and stiffness of the columns were changed to match the operational and environmental variability of real-world structures (States #2–#9). The operational variations were simulated by adding a mass, *m*, of 1.2 kg (nearly 19% of the total mass of each floor) to the base and to the first floor, as shown in Figure 3. The environmental variations were simulated by reducing one or more columns’ stiffness by 87.5%. This process was done by replacing the respective column with another one with half the cross-section thickness in the direction of shaking. The third group includes damaged state conditions simulated by introducing nonlinearities into the structure using a bumper and a suspended column, with different gaps between them, as shown in Figure 4-3. The gap between the bumper and the suspended column was varied (0.20, 0.15, 0.13, 0.10, and 0.05 mm) with the purpose of introducing different levels of nonlinearities (States #10–#14). Finally, the fourth group includes the state conditions with damage and operational and environmental changes (States #15–#17). For each of the seventeen state conditions, ten tests were performed so that the variability in the data could be taken into account. Therefore, for each of the five transducers, a total of ten time histories were considered in each state condition [2, 52].

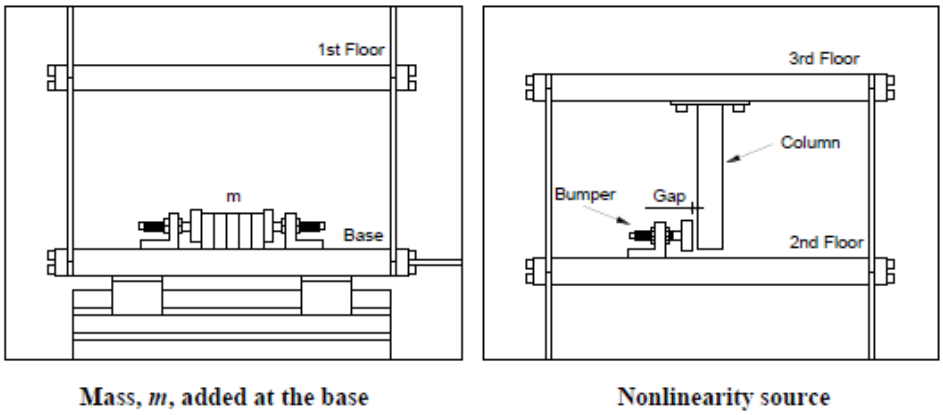

Figure 4-3: Structural details.

Table 1: Data labels of the structural state conditions.

Label	State Condition	Description
State #1	Undamaged	Baseline Condition
State #2	Undamaged	Mass = 1.2 kg at the base
State #3	Undamaged	Mass = 1.2 kg at the 1st floor
State #4	Undamaged	87.5% stiffness reduction in column 1 BD
State #5	Undamaged	87.5% stiffness reduction in column 1 BD and 1 AD
State #6	Undamaged	87.5% stiffness reduction in column 2 BD
State #7	Undamaged	87.5% stiffness reduction in column 2 BD and 2 AD
State #8	Undamaged	87.5% stiffness reduction in column 3 BD
State #9	Undamaged	87.5% stiffness reduction in column 3 BD and 3 AD
State #10	Damaged	Gap = 0.20 mm
State #11	Damaged	Gap = 0.15 mm
State #12	Damaged	Gap = 0.13 mm
State #13	Damaged	Gap = 0.10 mm
State #14	Damaged	Gap = 0.05 mm
State #15	Damaged	Gap = 0.20 mm and mass = 1.2 kg at the base
State #16	Damaged	Gap = 0.20 mm and mass = 1.2 kg at the 1st floor
State #17	Damaged	Gap = 0.10 mm and mass = 1.2 kg at the 1st floor

4.3. Feature Extraction

As mentioned before, the feature extraction process can be defined as the selection of features that allows one to distinguish between the damaged and the undamaged systems. The ideal approach for feature selection is to choose features that are very sensitive to damage and, for the most part, insensitive to other sort of effects, have the lowest dimension possible and also be extracted with minimal computational efforts. There are numerous methods to be employed in order to identify features for damage identification. In this section, an AR model will be used to extract features from the measured data as well as to determine the existence and location of damage in the test structure. Basically, this section will be a continuation of Figueiredo's work [2], where he attempted to determine the existence of damage using only data from Sensor 5. In this case, by using data from all accelerometers (Sensor 2-5), the author will attempt to determine the presence and location of damage.

The first step, to successfully apply AR models, is to identify the optimal number of parameters needed to fit the data. To that purpose, the AIC, as described in Chapter 3, will be applied to data from all the four accelerometers. Figure 4-4 shows the averaged AIC functions obtained using the data from the ten tests of the first nine state conditions (undamaged conditions, State #1-9) of each sensor. Note that, in theory, the optimal number is given by the minimization of the AIC function.

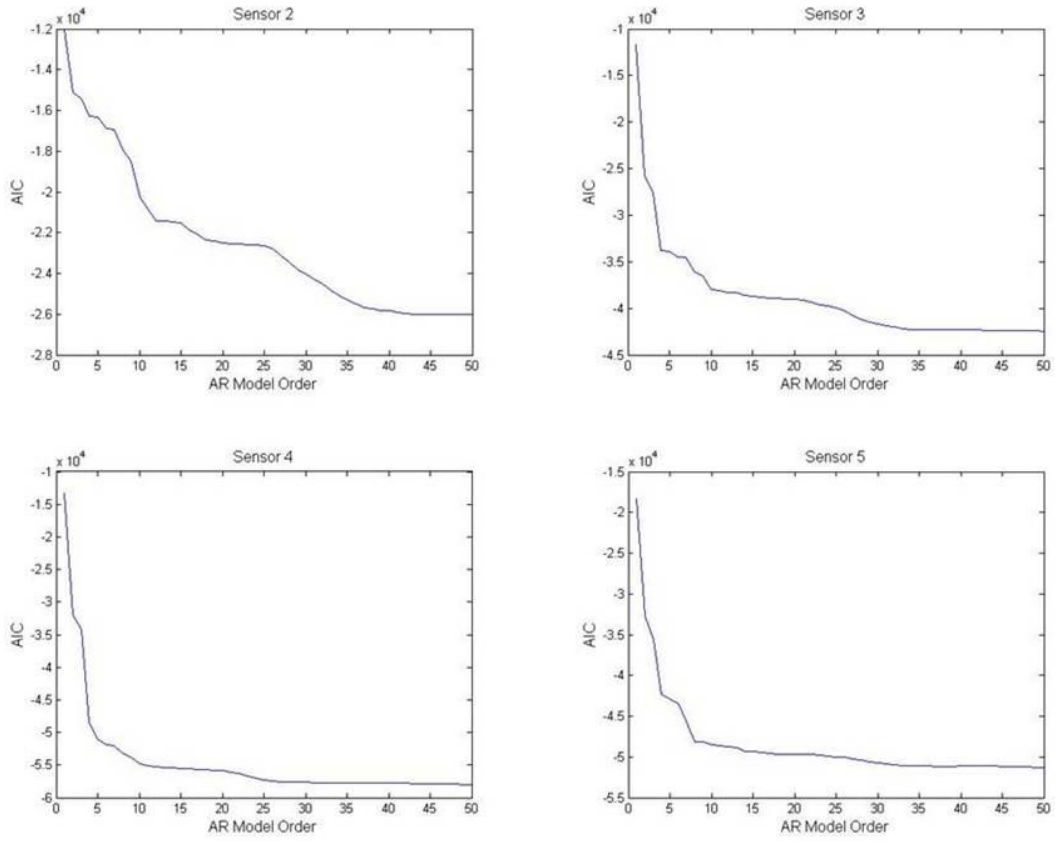

Figure 4-4: AIC functions of Sensors 2 to 5.

Even though it is not possible to establish a single solution for all accelerometers, the results suggest that, for the most part, the AIC functions start to converge for model orders between 20 and 40, which is an indication that the optimal common model order might be within that range. Based on this analysis, an AR(25) model will be used throughout this section. Note that it is not advisable to generalize model orders because each data set has its own internal structure and complexity. However, by doing so it will be possible to study the influence of model order on the damage detection.

After the selection of the AR model order, the AR parameters are estimated by fitting the AR(25) model to the time histories from Sensors 2 to 5, for all state conditions, using the

least-squares technique available in the SHMTools – software developed by the Engineering Institute from the LANL [56]. Figure 4-5 shows the AR parameters set into two main groups: the ones that correspond to the undamaged condition (State#1-9) and the ones that correspond to the damaged condition (State#10-17). The results show that the AR parameters themselves can be used directly as damage-sensitive features. When comparing the two groups, both figures suggest that upon the presence of damage, the AR parameters tend to decrease in amplitude. Furthermore, the results obtained from Sensor 4 show a clear distinction between the damaged and the undamaged states, which can mean that this sensor is more sensitive to the presence of damage than the other ones, as it is located close to the source of damage. However, one should note that Sensor 3 has opposed changes, which might be a result of the internal structure of the data.

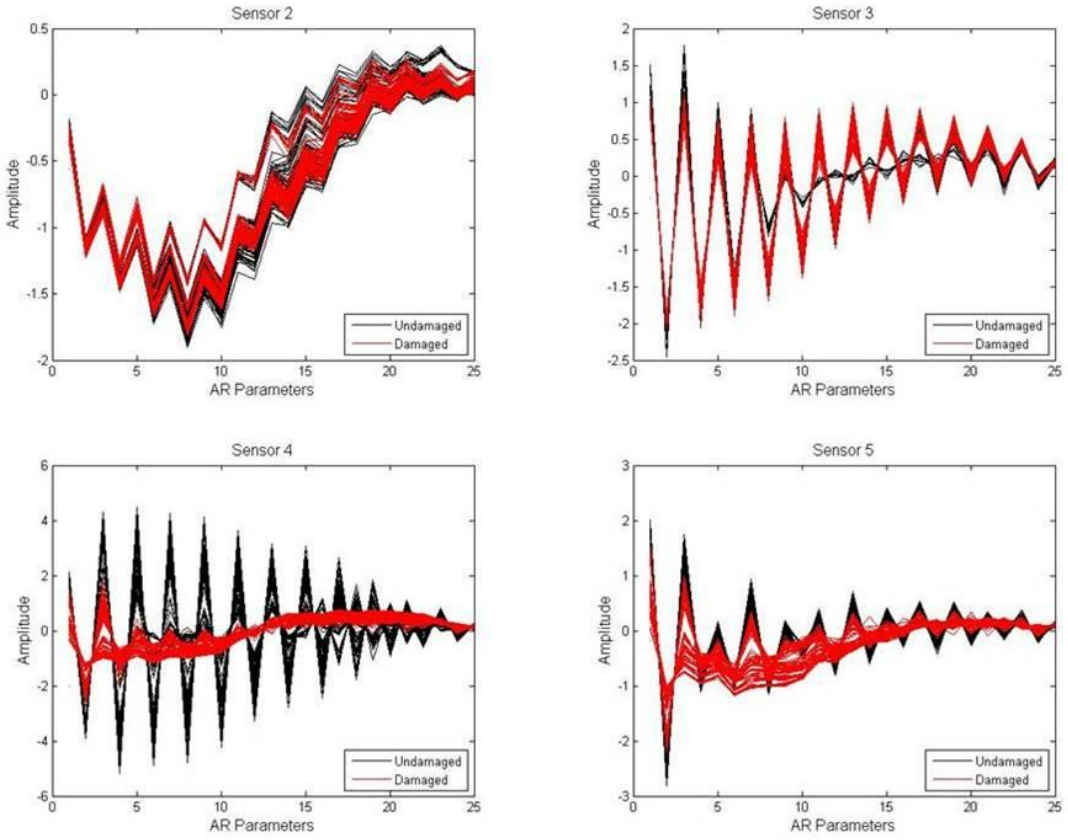

Figure 4-5: AR parameters Sensors 2 to 5.

Before the statistical modeling for feature classification stage and, in order to have a better insight on the data, a normality test was performed. Normality tests are used to determine if a data set can be modeled by a normal distribution. By performing a Q-Q Plot (using MATLAB Statistics Toolbox), sample quantiles from the AR parameters were compared with theoretical quantiles from a normal distribution (Figure 4-6). Since the parameters from the

baseline condition are grouped into a 90x25 matrix, plotting all 25 columns would not be appropriate. Therefore only a few columns were selected for these plots, more precisely the first columns of each quarter of the total number of parameters (columns 1, 7, 13 and 19). The figure indicates that the data have an underlying normal distribution, as the plots are close to linear, with insignificant changes in the tails.

Note that the importance of performing this test resides on the fact that non-Gaussian distributed features might cause some false alarms during the damage detection stage, as the MSD-based algorithm used to determine DIs assumes that the training data have an underlying multivariate normal distribution.

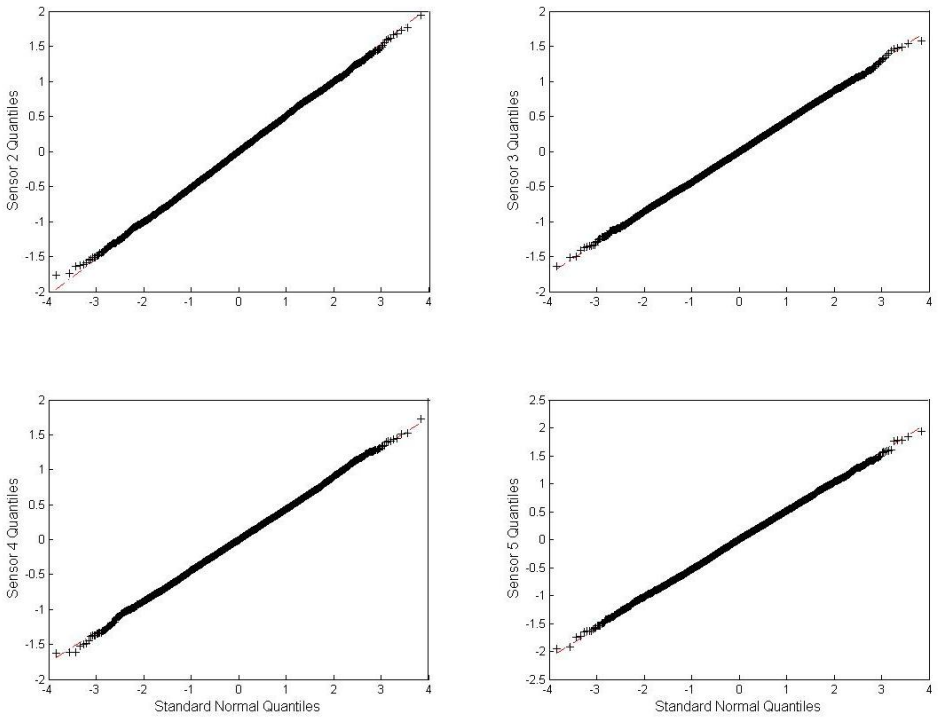

Figure 4-6: Q-Q plots from Sensors 2 to 5.

4.4. Statistical Modeling for Feature Classification

After the feature extraction process, the MSD-based algorithm was used to estimate DIs. As explained in the previous chapter, the MSD measures similarities between known and unknown sample sets. As the damaged and the undamaged states were known *a priori*, in the learning process, the mean vector and covariance matrix of the undamaged/reference condition were computed using data from the training matrix **X**. The training matrix is composed of all

data sets from the undamaged condition (State #1-9). Afterwards, the DIs were estimated based on the MSD-based algorithm, using the test matrix **Z** composed of all the data (State#1-17). For outlier detection, a threshold value was established based on a Chi-squared distribution (χ^2_{25}) with 25 DOF and for a level of significance equal to 5%. Note that from a statistical point of view, it represents the boundary between the undamaged and the damaged conditions. Figure 4-7 plots the DIs for all four accelerometers (Sensor 2-5) along with the thresholds.

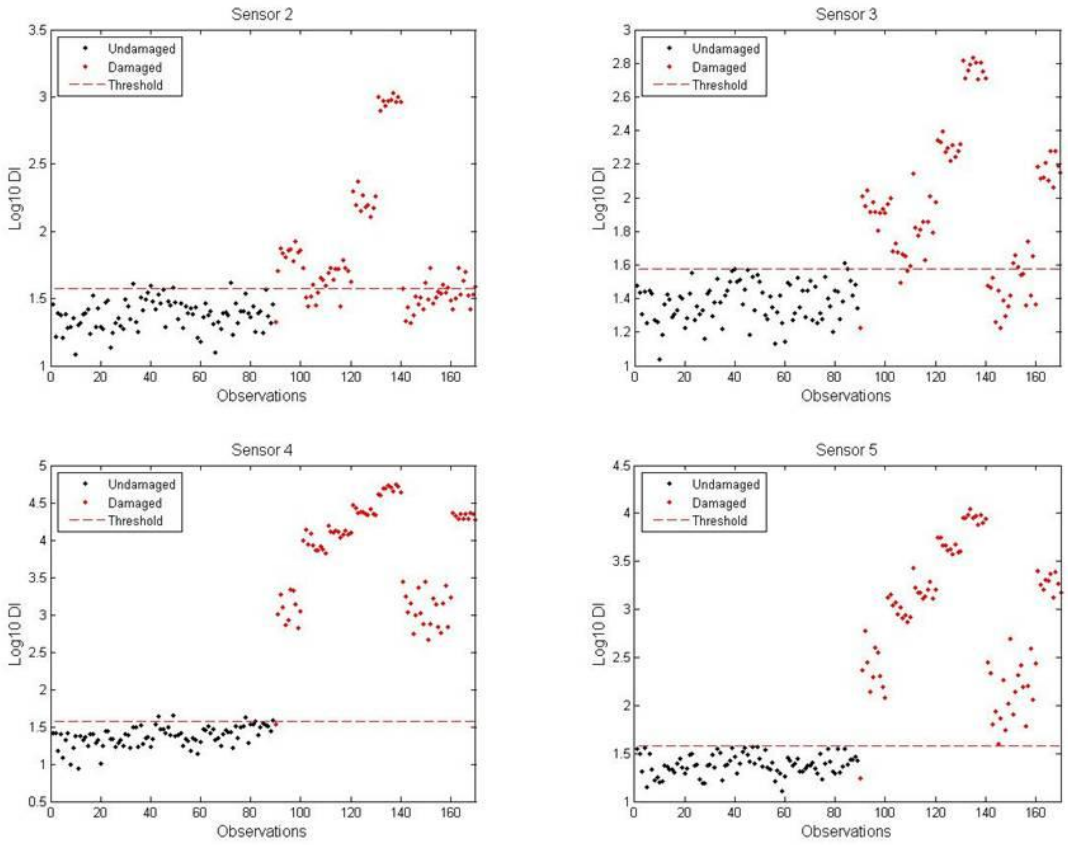

Figure 4-7: DIs for Sensors 2 to 5 using an AR(25) parameters as features.

From a general perspective, the results clearly show a difference in behavior upon reaching observations from State #10, which is when damage is introduced to the structure (by reducing the gap between the suspended column and the bumper), giving some indications that the attempt to determine the presence of damage was successful. Nonetheless, both Sensor 4 and Sensor 5 reveal a better classification performance, as most of the DIs from 91-180 are beyond the thresholds.

By carrying out a sensitivity analysis, the thresholds can also be used to determine the location of damage. By counting the number of DIs beyond the threshold, it is possible to estimate which sensor is closer to the source of damage. In Figure 4-8, one observes that the

number of outliers per sensor points out the location of the source of damage somewhere between Sensors 4 and 5, i.e. between the 2nd and 3rd floor, with a slitter tendency to Sensor 4, which is where the suspended column and bumper are actually located.

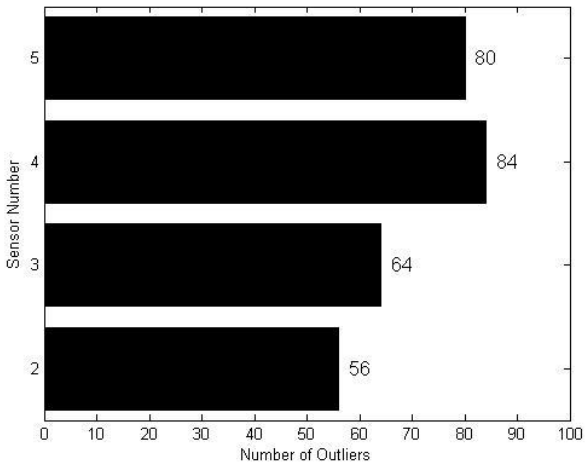

Figure 4-8: Number of outliers per sensor.

As mentioned previously in Chapter 3, false alarms of damage fall into two categories: (i) false-positive or Error Type I (the SHM system indicates damage when there is no damage) and (ii) false-negative or Error Type II (the SHM system gives no indication of damage when damage is present). In this study, as shown in Table 2, it was possible to determine the number and the type of errors associated with the feature classification technique used.

Table 2: Classification performance based on the number of false alarms.

Sensor	Error Type I (false-positive)	Error Type II (false-negative)
5	0	0
4	4	0
3	1	17
2	4	28

The high number of false alarms in Sensors 2 and 3 might be a direct result of an unsuitable model order (besides the fact that they are located far away from the source of damage). In order to point out the influence of the model order, a new AR model, AR(45), was used for these two sensors. The new model order was selected based on Figure 4-4, where it is possible to visualize that both AIC functions clearly converge at 45. Figure 4-9 plots the new

DIs for Sensors 2 and 3 by using the test matrix. These results clearly show a higher precision level when compared to the previous ones in Figure 4-7.

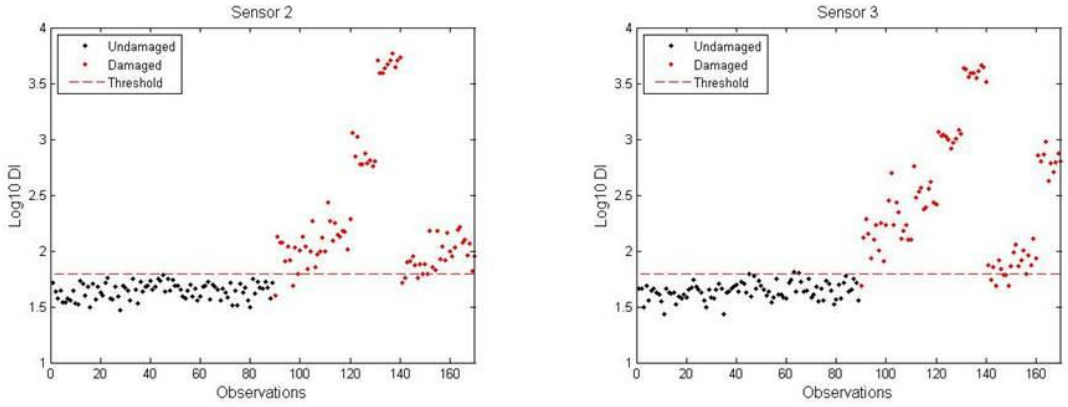

Figure 4-9: DIs for Sensors 2 and 3 using the AR(45) parameters as features.

The number of false alarms was significantly reduced, especially Error Type II showing improvements in the range of 70-86% for Sensors 3 and 2 respectively, as shown in Table 3.

Table 3: Classification performance based on the number of false alarms.

Sensor	Error Type I (false-positive)	Error Type II (false-negative)
3	3	5
2	0	4

In order to gain insight about the influence of the AR model order on the classification performance, Figure 4-10 plots, for both Sensors 2 and 3, the variation of the two types of errors as the model order increases from one to 60. The Error Type I (false-positive) show small and inconsistent variations as the model order increases, until it reaches a value (model order of 42) where no more errors of this type occur. For the Error Type II (false-negative), the lowest model order, AR(1), represents the maximum number of possible errors, 80, which is the total number of tests from the damaged states. The bottom line is that for low model orders, there are too few parameters to properly define the data and, as a result, the AR parameters are too wide and unable to detect damage. As the model order increases, the AR models are better adjusted to the data and they can more easily distinguish the damaged from the undamaged state conditions. Actually, these results also justified the optimal model order (45) suggested by the AIC.

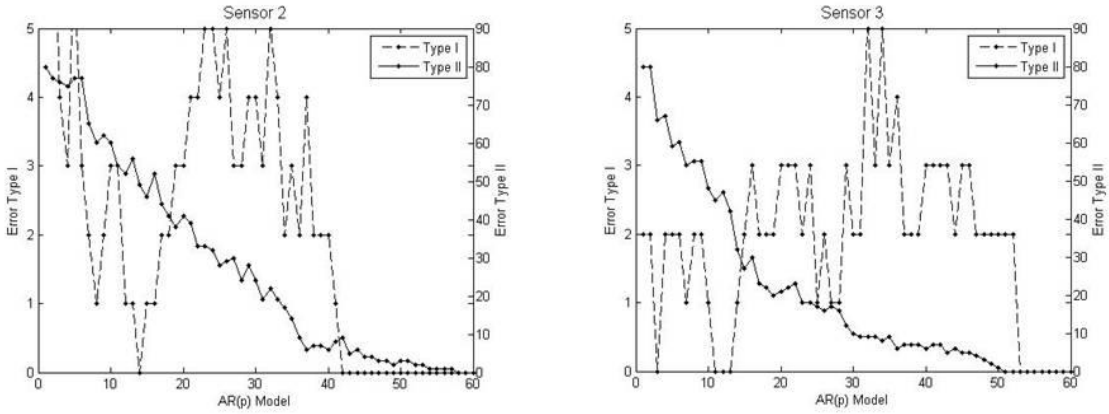

Figure 4-10: Error evaluation from Sensors 2 and 3.

Regardless of the AR model order differentiation for Sensors 2 and 3, the number of outliers still points out, although not as clearly as before, that the source of damage is located between Sensors 4 and 5, i.e. between the 2nd and the 3rd floor, as shown in Figure 4-11. This result suggests that if one uses the optimal AR model order, for each sensor, as suggested by the AIC, then it is possible to locate damage in the structure by performing some sort of sensitivity analysis.

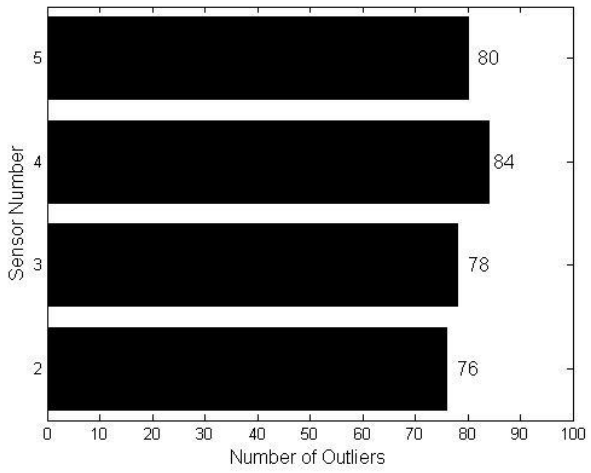

Figure 4-11: Number of outliers per sensor with AR(25) models for Sensors 4 and 5, and AR(45) for Sensors 2 and 3.

4.5. Conclusions

The objective of this chapter was to apply the SPR paradigm for SHM on data sets acquired from a base-excited three-story frame structure, created and tested in a laboratory environment at LANL. In the context of the hierarchical structure of damage identification, this

chapter was focused on determining the existence and, to the best extent, the location of damage in the structure. To that purpose, several statistical procedures were used to perform feature extraction and statistical modeling for feature classification.

In the feature extraction process, AR models were used to extract features from the measured data in the attempt to determine the presence of damage in the test structure. The estimated parameters of the AR models were directly used as damage-sensitive features. It was found that as damage was introduced to the test structure, in general the amplitudes of the AR parameters decreased, showing that these parameters are very sensitive to the presence of damage.

The statistical modeling for feature classification was carried out by using the MSD-based algorithm to estimate DIs and classify the damage-sensitive features. Even though the damaged and the undamaged states were known *a priori*, the algorithm was implemented using an unsupervised learning approach by using the undamaged states to train the algorithm and then applying all the data sets to test it. A threshold value was established using a Chi-squared distribution with a 95% confidence interval, in order to separate the DIs into damaged and undamaged conditions. In general, and probably due to the reduced size of the structure, the results showed that one could detect the presence of damage using only data from one sensor. In addition, the results showed that if one uses the optimal AR model order, for each sensor, as suggested by the AIC, then it is possible to locate damage in the structure by performing some sort of sensitivity analysis at the sensors' level. Basically, by counting the number of outliers beyond the thresholds in each sensor, one might set up a correlation between the number of outliers and sensors' location in the structure, to identify the localization of the source of damage.

5. APPLICABILITY OF THE SPR PARADIGM: Z24 BRIDGE

5.1. Introduction

In this chapter, the applicability of the techniques described in Chapter 3, and already applied in Chapter 4, to extract damage-sensitive features from the raw data, to remove the operational and environmental variability from those features, and to classify them into damage and undamaged conditions, will be tested on data from a real-world bridge, namely the Z24 Bridge in Switzerland. This bridge is part of a worldwide known project, which has been studied by some of the top researchers in the SHM field, in order to prove the feasibility of vibration-based health monitoring in civil engineering infrastructures. For almost one year, the Z24 Bridge was closely monitored before it was artificially damaged and later demolished. During that period, the influence of the environmental conditions, such as air humidity, wind and, most importantly, temperature, on the bridge's eigenfrequencies and mode-shapes was studied [57, 58]. The aim of the progressive damage tests, following the one-year long monitoring, was to recreate realistic and relevant damage scenarios in order to prove the hypothesis that damage can be detected, localized and even quantified by taking into consideration changes in the dynamics of the structures, especially based on damage-sensitive features such as eigenfrequencies and mode-shapes.

5.2. Structural Description and Data Acquisition

The Z24 Bridge, built between 1961 and 1963, was an overpass of the national highway A1 that linked Bern and Zurich, Switzerland. It was a post-tensioned concrete box girder bridge with a main span of 30 meters and two side-spans of 14 meters that crossed the A1 at a slight oblique angle (Figure 5-1) [57]. The two central supports were concrete piers connected to the girder, while both abutments were triple concrete columns connected via concrete hinges to the girder. Although it had no structural problems the bridge was demolished at the end of 1998 due to a new railway, adjacent to the highway, which required a larger side span [3, 34, 59].

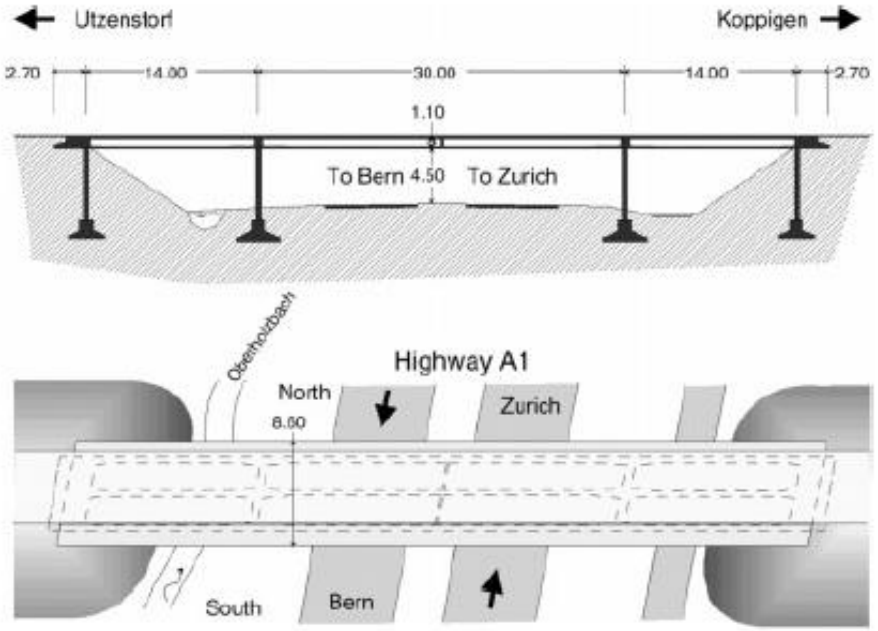

Figure 5-1: The Z24 Bridge cross section and top view.

Before its complete demolition, the bridge was subjected to three types of testing: (1) a long-term continuous monitoring test, which took place during the year before demolition and aimed to quantify the effects of the environmental variability on the bridge dynamics, (2) short-term intermittent monitoring tests, which were used to compare results from different excitation types and system identification methods, and (3) progressive damage tests, which took place a month before demolition and aimed to study the influence of realistic damage scenarios on the bridge dynamic properties. This project was unique in the sense that it allowed long-term continuous monitoring tests combined with realistic short-term progressive damage tests [3, 34, 57, 59].

5.2.1.Excitation Sources

Vibration-based damage detection methods are widely used among SHM researchers. This technique uses changes in the dynamic characteristics of a structure (i.e., eigenfrequencies, mode shapes, and damping properties) as indicators of damage. Since the dynamic characteristics of a structure are directly related to its physical properties, measured changes can be used to detect damage. In order to achieve this, various sources of dynamic excitation can be used, including forced excitation using a shaker and impact excitation by a falling weight or by using an impact hammer. There are other types of impact excitation referred to as free vibration testing. Some of these methods can be quite original, for example, in order to vertically excite

the Vasco da Gama Bridge in Lisbon, Portugal, Cunha et al. used a sudden release of a suspended boat beneath the bridges deck [34, 57].

In the last couple of years more attention has been given to ambient excitation, which is the structural response to the bridges to natural sources, such as traffic, wind or river flow among others. There are clear benefits of using these sources, such as being easily accessible, free, and being more representative of the actual excitation to which the bridge is subjected during its lifetime. However, due to the nature of the force itself, the input that these sources provide is very difficult to quantify, which introduces a certain level of uncertainty into the identification of the vibration mode parameters.

The excitation sources used on the Z24 Bridge tests can be divided into two parts. The first part took place the year before demolition and was mainly based on ambient excitation. During this time the bridge remained open to traffic so the ambient sources acting on the bridge were highway traffic, wind, and pedestrians. The second part occurred in the month before demolition. Since several damage scenarios were going to be applied, for safety reasons the bridge was closed to traffic. After the application of a damage scenario, an ambient and a shaker tests were performed. For the shaker tests, two shakers were used, one located at a sidespan, and the other at the mid-span. After damage scenario 8, in addition to the test already being made, a drop weight, located at mid-span, was also used to excite the bridge (details regarding the damage scenarios can be seen in Subsection 5.2.3). Figure 5-2 exemplifies the excitation sources used on the Z24-Bridge [34, 57].

Figure 5-2: Excitation Sources of the Z24 Bridge: on the left the highway traffic, in the middle the installation of a mass shaker and on the right the drop weight system.

5.2.2.Long-term Continuous Monitoring Test

The aim of the long-term continuous monitoring test, which was held from 11 November 1997 to 11 September 1998, was to quantify the environmental variability of the bridge dynamics. To that purpose all environmental variables that influenced the bridge dynamics had to be monitored. Therefore, sensors to measure air temperature, humidity, wind speed, wind direction and rain were installed at the bridge.

It is known that temperature variations have an influence on the dynamic behavior of a structure, as mention in Chapter 3. In addition, as the Z24's girder was a continuous beam, thermal variations may have lead to constraints which in turn could influence the Z24's dynamic behavior[3]. Therefore, a strategically distribution of temperature sensors was made over the girder to monitor the bridge's thermal state at three different locations: one in the main span and two in the side spans. The measurements were taken by eight thermocouples located at the center of the north (TWN), central (TWC) and south (TWS) web; below the north (TSWN) and south (TSWS) sidewalk; at the top (TDT) and soffit (TDS) of the deck, and at the soffit (TS) of the girder (Figure 5-3) [34, 57, 58].

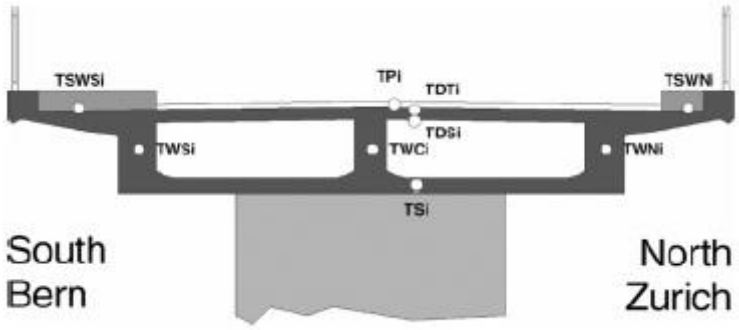

Figure 5-3: Cross section of the girder, showing the location where the temperature was monitored

While drilling access holes for the installation of the temperature sensors, it was discovered a cover of 16-18 cm of asphalt layer instead of 5 cm as indicated by the original blueprints. As a result, the temperature of the pavement (TP) was also measured at the middle of the three spans (Figure 5-3).

[3] Generally, when an object is subjected to a temperature variation (is heated or cooled) its length suffers a variation proportional to its original length. This phenomenon is called linear thermal expansion. If the object is not free to expand or contract its change in length can cause stress large enough to damage the object or to cause a change in its boundary conditions. In the Z24 bridge case, since the bridge girder was a continuous beam these problems could easily surface which would affect the bridges dynamic behavior.

Changes of dynamic soil stiffness can also result in variations of dynamics properties. Consequently, the soil temperature near each column was monitored, as well as near the north, central, and south parts of the intermediate piers resulting in a total of 12 sensors. To monitor dynamic behavior of the bridge, 16 accelerometers were placed across the structure at different locations and in different directions.

During the long-term continuous monitoring test data were acquired at hourly intervals. Every hour parameters such as air temperature, humidity, bridge expansion, wind characteristics, and soil and bridge temperatures were collected. In addition, every hour for 11 min, a group of the 16 accelerometers captured the vibrations of the bridge. All this information was later stored to a hard disk after compression. Due to the construction works at the new bridge, six temperature sensors were loss and one accelerometer was damaged. Even though the type of accelerometers used was specially designed for long-term monitoring, some revealed a considerable deterioration and some even failed during operation [34, 57, 58].

5.2.3.Progressive Damage Tests

The purpose of the progressive damage tests was to study how certain damage scenarios influenced the bridge dynamics. To achieve that, the selected damage scenarios had certain common characteristics: (i) be relevant for the safety of the bridge, i.e. if damage were to occur and went untreated it would endangered the bridges bearing capacity, (ii) the simulated damage occurred frequently and accordingly to the literature and experience of Swiss bridge owners, and (iii) be applicable to the Z24 bridge. With that in mind, a first selection of valid damage scenarios was made, some of which were later discarded based on limited time issues and safety requirements. The window time available for applying the damage scenarios was limited by the opening of the new bridge and the complete demolition of the Z24 Bridge. Since the A1 highway, which crossed the Z24 Bridge from underneath, was never closed to traffic some of the initial damage scenarios could not be applied without risking the safety of the traffic, which was considered of vital importance. For the same reason during these tests the traffic on the Z24 Bridge was diverted to another highway. Table 4 summarizes all progressive damage tests. Some of these tests are illustrated in Figure 5-4 [34, 57].

The first step prior to the implementation of the damage scenarios was to perform a reference measurement. Afterwards, and after each damage scenario, the bridge was subjected to an ambient and a forced vibration test. The ambient tests were performed during rush hour in the A1 highway, which crossed the Z24 Bridge from underneath, in order to increase the number of ambient excitation sources acting of the bridge. The other sources were wind and

walking of test crew. The forced vibration tests followed the ambient tests. For this test, two vertical shakers of EMPA Federal Laboratories, Switzerland, were used, namely one in a side-span and the other at mid-span. The input signals generated by the shaker were calculated using an inverse fast Fourier transform algorithm and ranged between 3-30 Hz. Due to the limited number of accelerometers and acquisition channels, the structure was measured in nine setups using five reference channels. After damage scenario 8, a drop weight test was included in the test. In the end, a total of 65 536 samples were collected at a sampling rate of 100 Hz [34, 57].

Table 4: Progressive damage tests.

No.	Data (1998)	Scenario	Description/simulation of real damage case
1	04.08	First reference measurement	Healthy structure
2	09.08	Second reference measurement	After installation of lowering system
3	10.08	Lowering of pier, 20 mm	Settlement of subsoil, erosion
4	12.08	Lowering of pier, 40 mm	
5	17.08	Lowering of pier, 80 mm	
6	18.08	Lowering of pier, 95 mm	
7	19.08	Tilt of foundation	Settlement of subsoil, erosion
8	20.08	Third reference measurement	After lifting of the bridge to its initial position
9	25.08	Spalling of concrete, 24 m^2	Vehicle impact, carbonization, and subsequent corrosion of reinforcement
10	26.08	Spalling of concrete, 12 m^2	
11	27.08	Landslide of abutment	Heavy rainfall, erosion
12	31.08	Failure of concrete hinge	Chloride attack, corrosion
13	02.09	Failure of anchor heads I	Corrosion, overstress
14	03.09	Failure of anchor heads II	
15	07.09	Rupture of tendons I	Erroneous or forgotten injection of tendon tubes, chloride influence
16	08.09	Rupture of tendons II	
17	09.09	Rupture of tendons III	

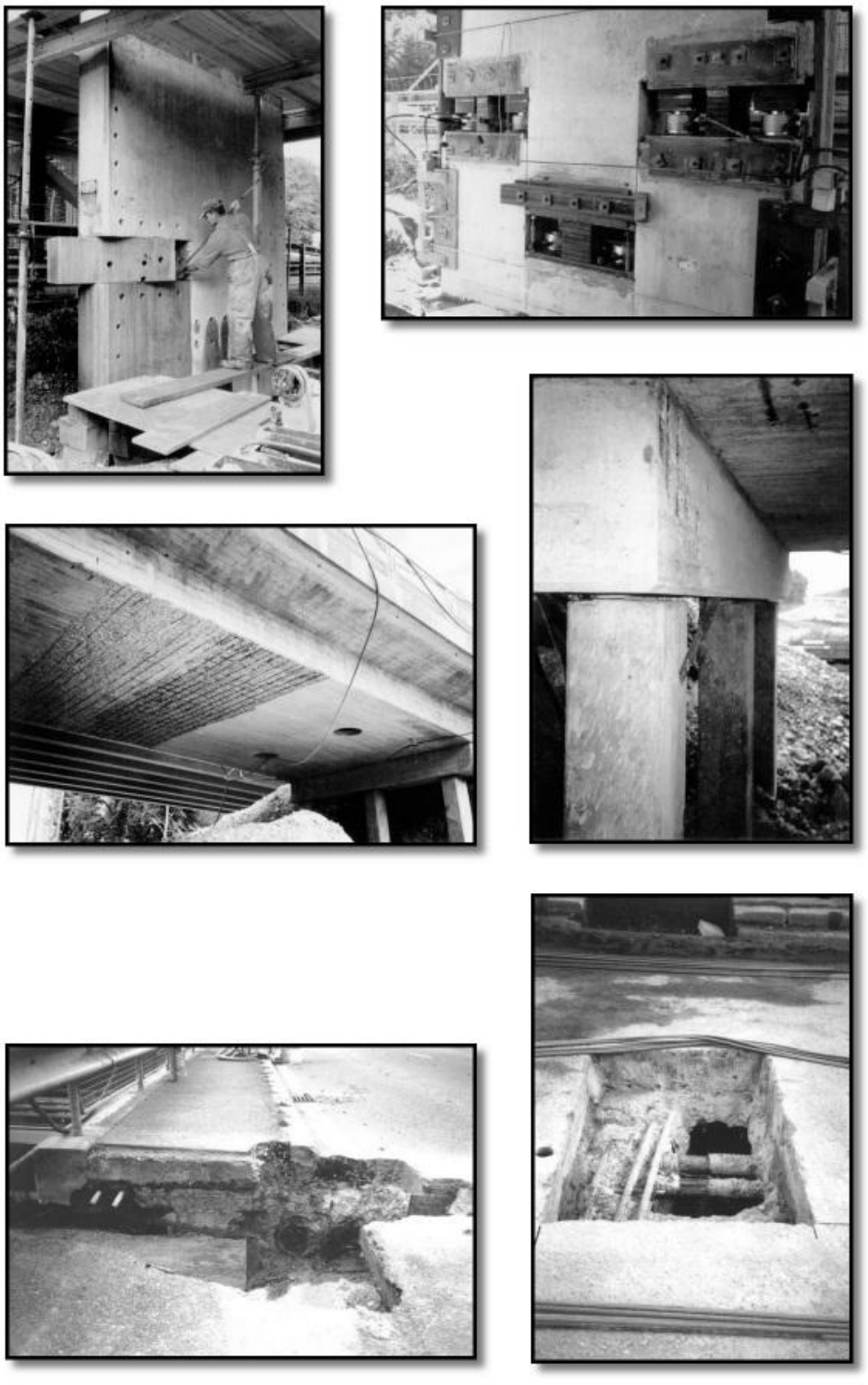

Figure 5-4: Photographs illustrating the applied damage scenarios. From left to right and from top to bottom: (1) cutting of a pier to install the settlement system, (2) settlement system, (3) spalling of concrete, (4) failure of a concrete hinge, (5) failure of anchor heads, (6) failure of tendon wires.

5.3. Feature Extraction

For this study, a total of 235 observations were taken into account, which correspond to daily feature vectors composed of the first three natural frequencies estimated at 5am (because of the lower differential temperature on the bridge). These feature vectors were extracted by Figueiredo et al. using an automatic modal analysis procedure based on the frequency domain decomposition [60, 61]. (Note that this procedure was only capable of estimating with high reliability the first three frequencies.) During the extraction process, it was noticed that the first and the third natural frequencies were strongly correlated (with a correlation coefficient of nearly 0.94 as summarized in Table 5), which allows one to perform, if necessary, dimension reduction of the extracted feature vectors from three to two. From the 235 observations, the first 197 ones correspond to the healthy state of the bridge (baseline condition) which, chronologically, lasts from 11th of November 1997 to 3rd of August 1998 while the remaining 38 ones correspond to the progressive damage testing period, lasting from 4th of August to 10th of September 1998. Although the main goal was to monitor a whole year, the monitoring system was, occasionally, not operational during short periods. Therefore, only 235 measurements were successfully extracted. Figure 5-5 illustrates the first three natural frequencies and the ambient temperature as a function of time. Several frequency oscillations are visible as well as a distinct frequency increase during a period of time between observations 50 and 100. As it was referenced before, during this period damage had not been yet introduced in the structure. Thus, this phenomenon can only be explained by structural changes caused by operational and/or environmental effects, most likely by temperature variations. From the observation of the figures, it is also clear when the progressive damage testing starts as indicated by a tendency to drop down in the magnitude of each frequency. It is important to note that these tests were carried out in a sequence manner, resulting in an accumulative degradation of the bridge.

Table 5: Correlation matrix of the natural frequencies.

	$\mathbf{f_1}$	$\mathbf{f_2}$	$\mathbf{f_3}$
$\mathbf{f_1}$	1	0.77	0.94
$\mathbf{f_2}$	0.77	1	0.78
$\mathbf{f_3}$	0.94	0.78	1

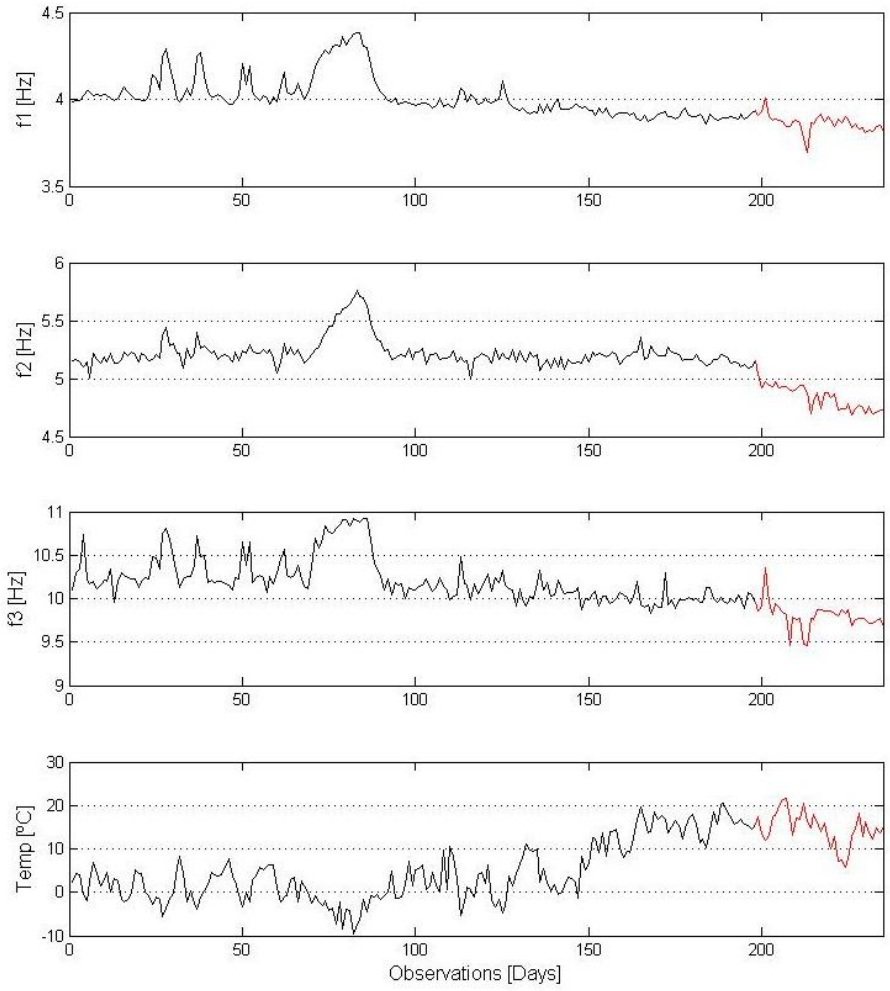

Figure 5-5: First three natural frequencies and ambient temperature.

As it is well known, temperature changes affect the Young's modulus of both concrete and asphalt, which will consequently affect the natural frequencies of the bridge. To better understand this relation, frequency-temperature graphics were developed. Figure 5-6 plots the 1st natural frequency versus the temperature of the deck soffit (TDS2) along with the 2nd natural frequency versus the temperature of the wearing surface (TP1). (Note that both temperature-sensor locations can be seen in Figure 5-3.) Upon analyzing both graphics, the relation between frequency and temperature can nearly be described as bilinear, as suggested by two imaginary straight lines converging around 0°C. During cold periods (temperatures below 0°C) the bridge stiffness changes significantly from the bridge stiffness in normal periods (temperatures above 0°C). (Note that this bilinear behavior is present itself in all combinations of frequency vs. temperature.) Peeters & De Roeck [3] claimed that those variations are mainly introduced by the asphalt layer. Basically, during cold periods, the asphalt layer considerably increases the stiffness of the structure, which in turn causes a variation of the natural frequencies.

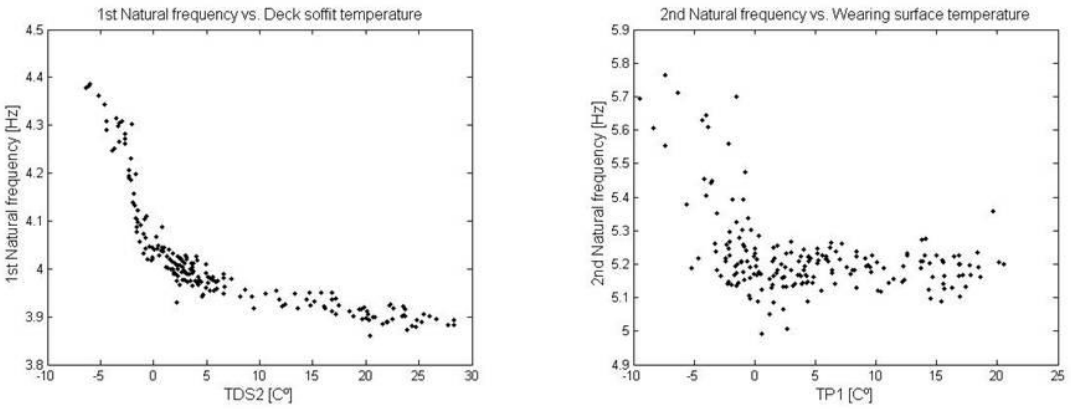

Figure 5-6: Natural frequencies versus temperatures.

In order to have a better insight on the data sets, a normality test was performed. By performing a Q-Q Plot, the sample quantiles of the different natural frequencies are compared with theoretical quantiles from a normal distribution. The main assumption is that if a natural frequency follows a normal distribution, the plot should be close to linear. Therefore, from Figure 5-7, one observes significant deviations on the tails of the distributions, which is an indication that the natural frequencies do not follow individual normal distributions.

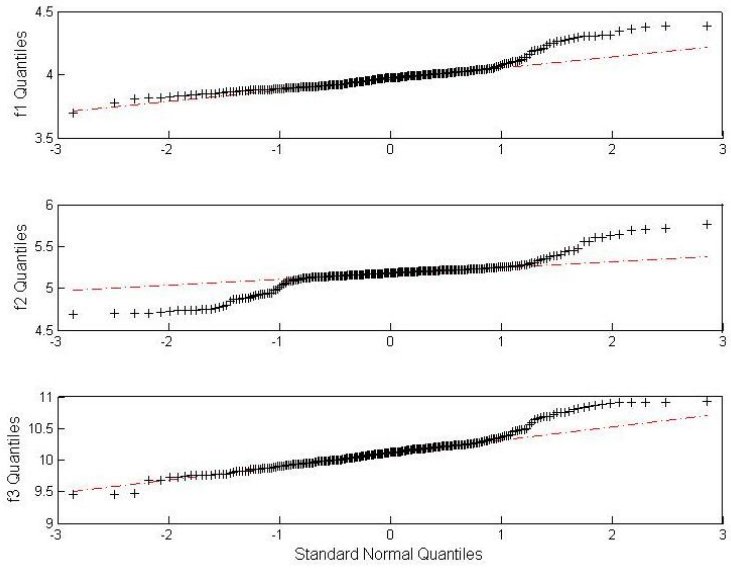

Figure 5-7: Q-Q Plot of the three natural frequencies.

As the gathered natural frequencies do not follow normal distributions, one can estimate the PDF of those using the *ksdensity* function available in MATLAB. Figure 5-8 shows several bumps in the individual PDFs, which suggest that the natural frequencies might follow a mixture of multivariate normal distributions rather than a unique standard multivariate normal

distribution. Note that the non-Gaussian distributed features might cause some false alarms during the damage detection stage, especially when classifiers make assumptions of normality, as will be shown later on.

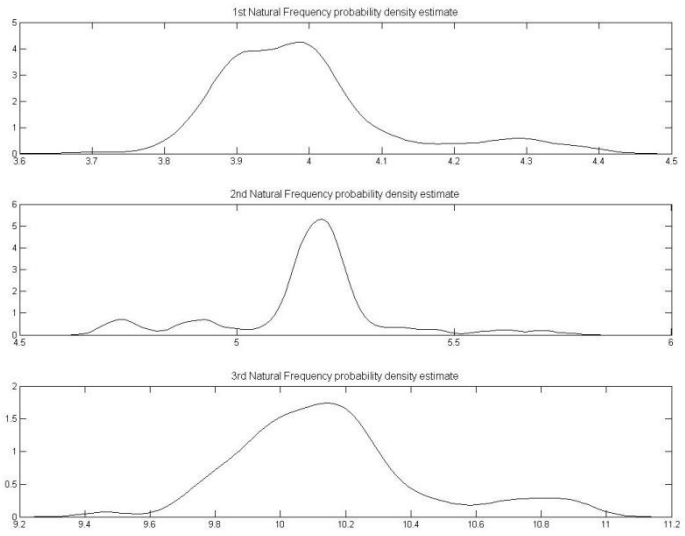

Figure 5-8: Individual probability density estimates of the three natural frequencies.

5.4. Statistical Modeling for Feature Classification

5.4.1. Outlier Detection based on a Multivariate Gaussian Distribution

The damage detection strategy was carried out similarly to the one in Chapter 4: the extracted feature vectors (or observations), in this case the first three natural frequencies, were divided into a training matrix **X**, composed of the entire undamaged observations, and a test matrix **Z**, composed of all observations available, i.e. both the undamaged and the damaged ones; afterwards, the classification is performed using the MSD-based algorithm, which assumes that the training data follow a multivariate normal distribution.

Basically, in the learning stage, the mean vector and covariance matrix of the baseline/reference condition were computed using the training matrix **X**. Afterwards, the DIs were estimated based on the MSD-based algorithm using the test matrix **Z**. A threshold value was also established using a Chi-squared distribution (χ_3^2) with three DOF and for a level of significance of 5%, in an attempt to differentiate the states from the damaged and the undamaged conditions.

Figure 5-9 plots the DIs derived from the test matrix. As one can visualize in the figure, the MSD-based algorithm triggers several non-random false alarms between observations 50 and 100, meaning that the algorithm indicates the presence of damage when in fact there is none. This fact highlights that the algorithm cannot get rid of the environmental effects. Moreover, Table 6 summarizes the total number of misclassifications (27) as well as of the number of Error Type I (false-positive) and Error Type II (false-negative). The high number of Errors Type I (19), which is higher than the tolerance (10) given by level of significance, might be related to the multimodality of the data, as a result of the bilinear behavior caused by the temperature variability. (Actually, this fact was predictable as mentioned in Subsection 5.3.) Note that the MSD-based algorithm assumes that the training data follow a multivariate normal distribution, which implies that it might not work properly when the training data assumes an underlying GMM.

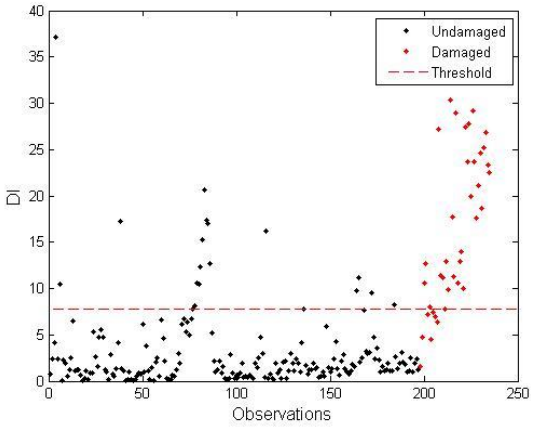

Figure 5-9: DIs derived from the MSD-based algorithm.

Table 6: Misclassifications derived from the MSD-based algorithm.

	Error Type I (false-positive)	Error Type II (false-negative)	Total number of False Indications
Multivariate Normal Distribution	19	8	27

5.4.2. Outlier Detection based on a Gaussian Mixture Model

With the aim of improving the feature classification performance, an algorithm based on a GMM was developed. This algorithm aims to: (1) determine the number, K, of normal components contained in the training data, (2) identify the parameters of each normal

component k (mean vector, covariance matrix, and weight factor), (3) construct a MSD-based algorithm for each normal component, and finally (4) for each observation, *i*, one must determine the minimum DI_i, i.e. $DI_i = min(DI_{I,k})_{k=1,..,K}$.

The backbone of this algorithm was the MATLAB's Gaussian mixture model *gmdistribution.fit* function, which can be found in MATLAB's Statistics Toolbox. This function uses an EM algorithm to produce maximum likelihood estimates of the various parameters in a GMM with K components. Basically, the idea is to input data from the Z24 Bridge, more specifically the training matrix **X** (composed solely of feature vectors from the undamaged condition), and determine the mean vector and the covariance matrix of each normal component that defines the mixture model. In order to achieve that, the number of components K must be determined prior to the data input.

Amongst its several properties, the *gmdistribution.fit* function possesses an AIC output variable. Therefore, it is possible to estimate the number of components that best fits the training data simply by analyzing the AIC values. Figure 5-10 plots the AIC function ranging from one to five components. It is important to note that every time the *gmdistribution.fit* function is run, the EM algorithm starts its process of iterations at a random point and, from there, it converges to the nearest local maximum of the likelihood. As a result, it is possible that the acquired point of convergence is a local maximum instead of the global maximum. In order to overcome this problem the *gmdistribution.fit* function was run several times in the attempt to converge to the global maximum. The values plotted in Figure 5-10 were determined using this process.

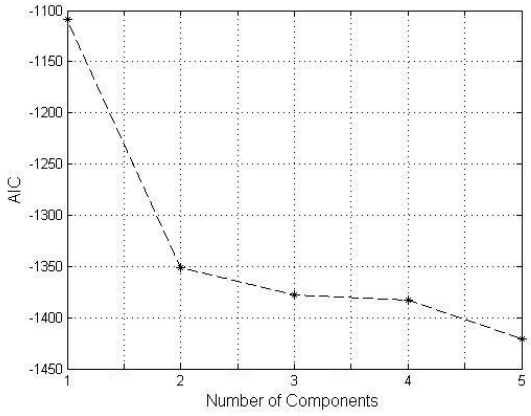

Figure 5-10: AIC function for mixture models ranging from one to five normal components and assuming first three natural frequencies.

Even though the AIC function is not minimized in that range, it is assumed that the appropriate number of components is in the range between two and four, because the AIC values start converging around those points. Nevertheless, with the purpose of studying the influence of the number of components on the classification performance, four different values were considered. Table 7 summarizes some parameters estimated as a function of the number of components.

Table 7: Estimated parameters varying the number of components, K=2-5.

	Components	**Weight (%)**	**Mean f_1 (Hz)**	**Mean f_2 (Hz)**	**Mean f_3 (Hz)**
K = 2	#1	80.9	4.0	5.2	10.1
	#2	19.1	4.2	5.4	10.6
K = 3	#1	74.2	4.0	5.2	10.1
	#2	10.3	4.3	5.5	10.8
	#3	15.5	4.0	5.2	10.3
K = 4	#1	10.1	4.3	5.5	10.8
	#2	6.7	4.0	5.1	10.2
	#3	73.0	4.0	5.2	10.1
	#4	10.2	4.1	5.3	10.4
K = 5	#1	12.9	4.0	5.3	10.4
	#2	6.8	4.0	5.1	10.2
	#3	18	3.9	5.2	9.9
	#4	51.9	3.9	5.2	10.1
	#5	10.4	4.3	5.5	10.8

After the extraction of all mean vectors and covariance matrices, MSD-based algorithms were used to estimate the DIs using the test matrix **Z**. Figure 5-11 plots the DIs for the four cases, along with a threshold established using a Chi-squared distribution (χ_3^2) with three DOF and for a level of significance of 5%, to differentiate the damaged from the undamaged observations.

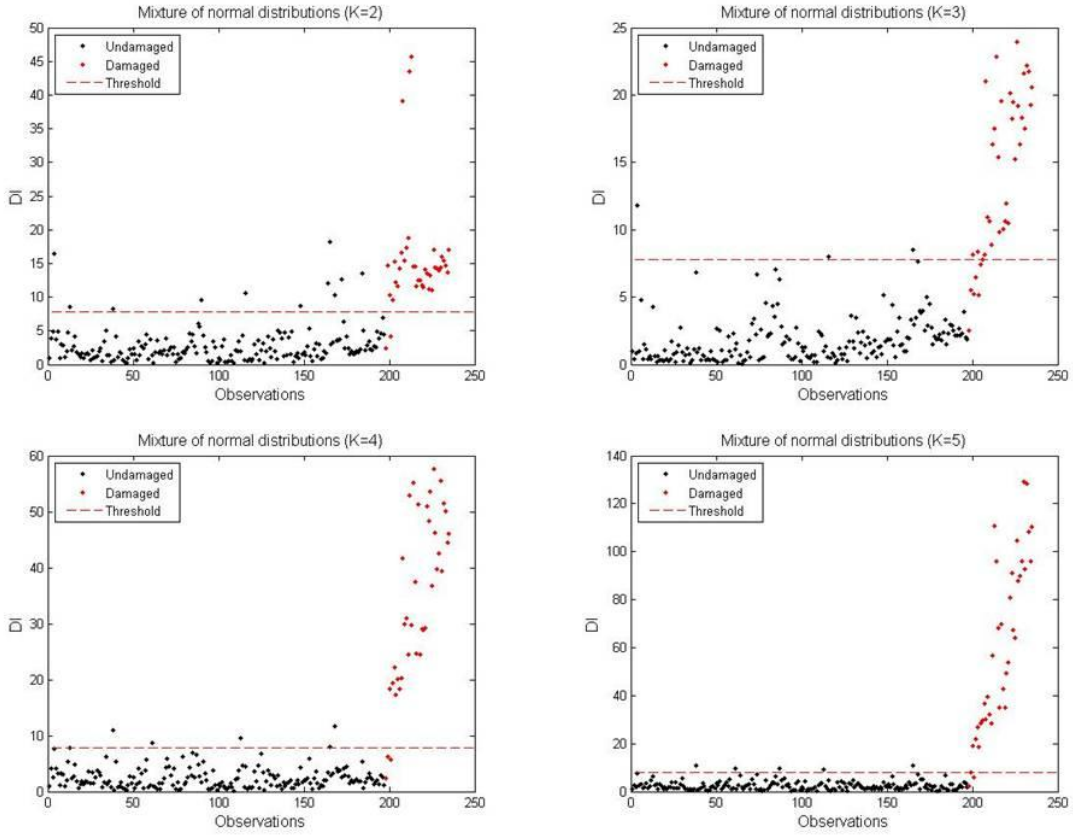

Figure 5-11: DIs for the different number of components (K=2-5).

Visually, and when comparing the results with the ones obtained assuming a unique multivariate normal distribution in the training process (Figure 5-9), the algorithm based on the GMM is more capable to differentiate changes caused by temperature variations from those changes caused by actual damage, as indicated by the apparently randomness of the DIs during the undamaged condition (1-197). Furthermore, Table 8 summarizes the classification performance (in terms of Error Type I and Error II) assuming a multivariate normal distribution (as shown in Table 6) and four independent GMMs with varying number of mixture normal components (K=2-5).

Table 8: Classification performance for different classifiers assuming three natural frequencies.

		Error Type I (false-positive)	Error Type II (false-negative)	Total number of False Indications
Multivariate Normal Distribution		19	8	27
Mixture of Normal Distributions	**K=2**	11	2	13
	K=3	3	7	10
	K=4	5	3	8
	K=5	5	2	7

The results obtained assuming a mixture of normal distributions show, in the worst case (K=2), a drop rate of more than 50% in terms of misclassifications when compared to the results assuming a multivariate normal distribution. Actually, the above classification results confirm the indications given by the AIC function as it converge for K=2. Even though the number of Type I and II errors appears to decrease in an unstable manner as a function of the number of components, it is clear that the total number of misclassifications is inversely proportional to the number of mixture components assumed in the GMM. However, one should note that high number of components might overfit the model, which is not convenient for generalization purposes. Actually, the model with K=2 seems to be appropriate as the number of Type I errors (11) is close to the tolerance (10) given by the level of significance.

In the feature extraction stage of this chapter (Subsection 5.3), it was addressed that during the extraction process, the first and the third natural frequencies were strongly correlated, which allows one to perform some sort of dimensionality reduction of the extracted feature vectors from three to two. For comparison purposes, the same procedure for feature classification was carried out by taking into account only the first two natural frequencies. Figure 5-12, Figure 5-13, and Table 9 show the AIC function, the DIs for the different number of components of the mixture models, and their respective classification performance.

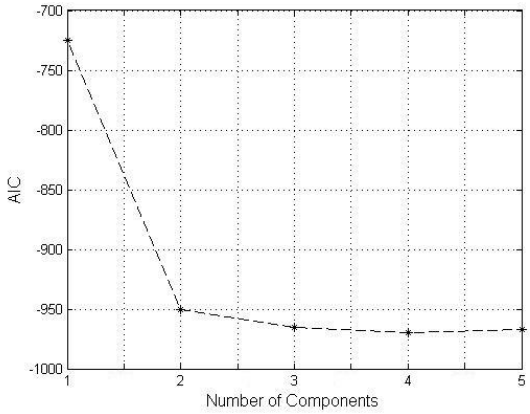

Figure 5-12: AIC function for mixture models ranging from one to five normal components and assuming only the first two natural frequencies.

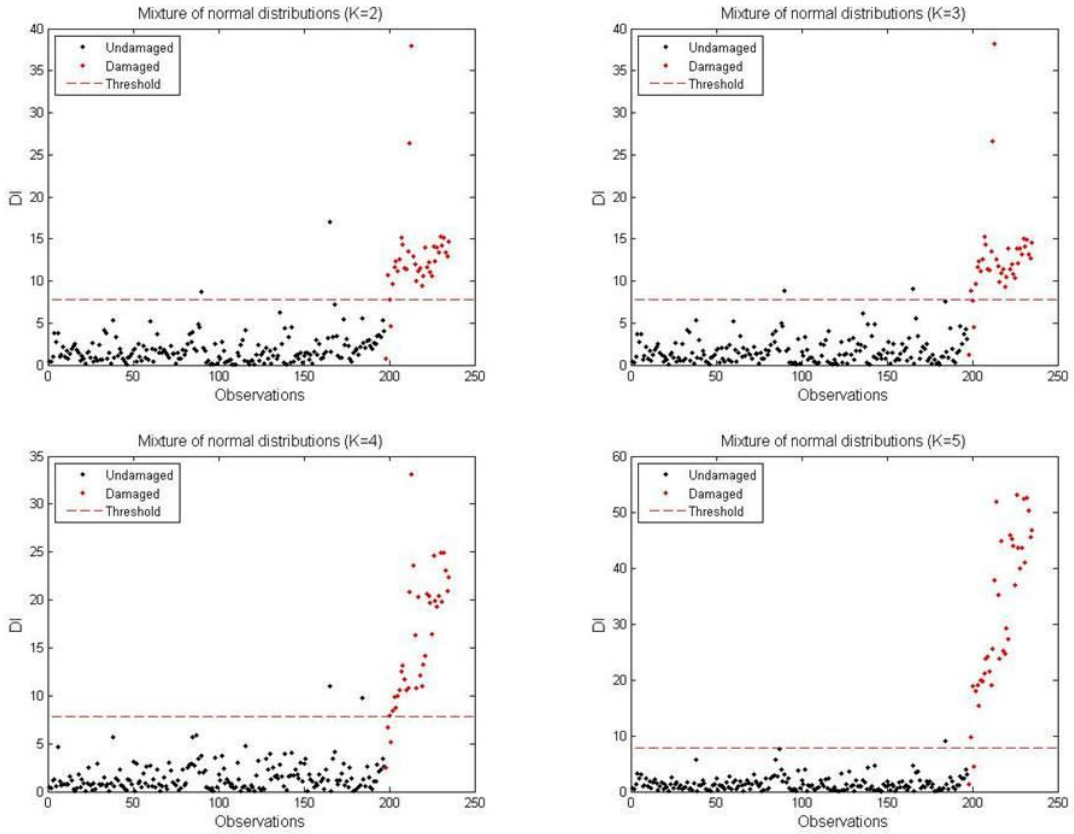

Figure 5-13: DI for the different number of components using only two natural frequencies.

Table 9: Classification performance for different classifiers assuming the first two natural frequencies.

		Error Type I (false-positive)	Error Type II (false-negative)	Total number of False Indications
Multivariate Normal Distribution		19	8	27
Mixture of Normal Distributions	**K=2**	2	3	5
	K=3	2	3	5
	K=4	2	3	5
	K=5	1	2	3

In terms of total number of misclassifications, the results obtained using only two frequencies were extremely good. Even for a low number of components, the numbers of false indications were far lower than the ones determined with three frequencies Furthermore, the results did not show any inconsistency over the increasing number of components, which is also indicated by a flat AIC function by K between two and five. After reaching five components, the algorithm became extremely accurate, as it has only three false indications of damage in a total of 235 observations (achieving a level of accuracy of 98.7%). Actually, this result highlights the importance to optimize the number and type of features used for feature classification. In the reality, high dimensional feature vectors might carry out more room to hide changes in the features caused by damage. However, it might be appropriate for generalization purposes as suggested the low number of Type I errors when compared to the tolerance given by the level of significance.

5.5. Conclusions

The goal of this chapter was to make the transition of the statistical pattern recognition paradigm for SHM from the laboratory environment to the field by applying it upon data sets acquired from a bridge in Switzerland – the Z24 Bridge. In the context of the hierarchical structure of damage identification, this chapter was mainly focused on determining the existence of damage by overcoming the problems imposed by the environmental and operational variations. To that purpose, a number of statistical procedures were tested to treat the acquired data.

The feature extraction stage permitted to unveil the existence of unusual oscillations in first three natural frequencies. These oscillations were later correlated to cold periods, during

which temperatures reached levels below 0°C, causing a tremendous increase in the stiffness of the asphalt layer which, in turn, caused a variation of the natural frequencies. By plotting the different eigenfrequencies versus temperature, a bilinear behavior with slop change around 0°C was discovered. In light of this discovery, a normality test was performed to determine if the natural frequencies follow a normal distribution. The results suggested that the natural frequencies follow a mixture of multivariate normal distributions rather than a unique standard multivariate normal distribution. This fact became an issue in the statistical modeling for feature classification stage, which led to concerning high level of false alarms. As a consequence, a new approach had to be considered, namely the use of GMM.

Actually, the effects of the environmental conditions on the Z24 Bridge reinforced the fact that field deployment of SHM systems needs to be accompanied by robust techniques to take them into account in the damage identification process. Environmental and operational effects often have a large influence on the measured dynamics response of a structure and, as it was explained before, damage detection is based on the premise that damage in the structure will cause changes in the materials and, consequently, causing changes in measured vibration data. Therefore, it is crucial to quantify the effects of changing environmental and operational conditions so that they cannot hide little changes in the system's vibration signal caused by damage.

Thus, with the aim of improving the feature classification performance, an algorithm based on a GMM was developed. This algorithm aims to: (1) determine the number, K, of normal components contained in the training data, (2) identify the parameters of each normal component k (mean vector, covariance matrix, and weight factor), (3) construct a MSD-based algorithm for each normal component, and finally (4) for each observation, *i*, one must determine the minimum DI_i, i.e. $DI_i = min(DI_{i,k})_{k=1,\ldots,K}$. In order to study the influence of the number of mixture normal components on the classification performance, four different models (with different number of components) were considered.

Firstly, assuming feature vectors composed by three natural frequencies, the comparison of the results from the GMMs with the ones obtained assuming a unique multivariate normal distribution, proved that the models, in terms of misclassifications, and in the worst case (K=2), permits a drop rate of more than 50%, proving that the GMM was more capable to differentiate changes caused by temperature variations from those changes caused by actual damage. The number of mixture components assumed in the GMM proved to be inversely proportional to the total number of misclassifications.

Secondly, for comparison purposes, the same procedure for feature classification was carried out by taking into account only the first two natural frequencies. In terms of total number of misclassifications (both Error Type I and Error II), the results obtained were better than for the case of three natural frequencies, even for a low number of components (K=2). However, the percentage of Type I errors, significantly lower than the level of significance,, suggests than the model with two natural frequencies is overfitted, and so it is not appropriate for general purposes.

In conclusion, and comparing the two algorithms for statistical modeling for feature classification used in this chapter, the one based on a GMM has shown to be more appropriate under severe changes caused by operational and environmental variability, especially when those changes impose a non-linear structure response. This chapter also permitted to conclude the applicability of this algorithm to detect local damage using global features extracted on vibration data.

6. SUMMARY, CONCLUSIONS AND FUTURE WORK

The Silver Bridge failure, in 1967, was the first of many catastrophic bridge failures that brought about the need for BMSs. Some of these disasters occurred in the USA, however, similar cases can be found all over the world. Even though tragic, these failures have sparked a worldwide interest in bridge safety. The investigation of each of these failures, and the knowledge gained from understanding the conditions on which they occurred, have helped the engineers to find ways to ensure that similar failures can be prevented in the future. As a result, new codes and regulations have been implemented and the SHM concept has been created as a way of improving BMSs. However, the collapses of the Hintze Ribeiro Bridge, in 2001, and more recently, in 2007, the I-35W Bridge over the Mississippi River brought once again bridge safety to the forefront of the public. Therefore, due to its potential, the SHM technology has received considerable attention in the last years, which permitted it to evolve and mature to the point where few attempts of integrated SHM systems already exist.

Herein, the SHM process is posed in the context of the SPR paradigm, which can be broken down into a four-stage process: (1) Operational Evaluation, (2) Data Acquisition, (3) Feature Extraction, and (4) Statistical Modeling for Feature Classification. Although addressing all aspects of the paradigm, this dissertation was mainly focused on feature extraction and on the development of models for feature classification stages.

In Chapter 4, the applicability of the SHM-SPR paradigm for damage identification was tested on standard data sets acquired from a base-excited three-story frame structure. Several statistical procedures were used in order to perform feature extraction and statistical modeling for feature classification.

In the feature extraction process, AR models were used to extract features from the measured data in the attempt to determine the presence and location of damage in the test structure. The estimated parameters of the AR models were directly used as damage-sensitive features. The AR model proved to be a useful feature extraction technique, as its parameters were shown to be very sensitive to the presence of damage.

The statistical modeling for feature classification was carried out by using the MSD-based algorithm to estimate DIs and classify the damage-sensitive features. Even though the damaged and the undamaged states were known *a priori*, the algorithm was implemented using an unsupervised learning approach by using the undamaged states to train the algorithm and then applying all the data sets to test it. A threshold value was established using a Chi-squared

distribution with a 95% confidence interval, in order to separate the DIs into damaged and undamaged conditions. In general, and probably due to the reduced size of the structure, the results showed that one could detect the presence of damage in the structure using only data from one sensor. In addition, the results showed that if one uses the optimal AR model order, for each sensor, as suggested by the AIC, then it is possible to locate damage in the structure by performing some sort of sensitivity analysis in each sensor. Basically, by counting the number of outliers beyond the thresholds in each sensor, one might set up a correlation, between the number of outliers and sensors' location in the structure, to identify the localization of the source of damage.

In Chapter 5, the SHM-SPR paradigm was tested on data from a real-world bridge, namely the Z24 Bridge, in Switzerland. In the context of the hierarchical structure of damage identification, this chapter was only focused on determining the existence of damage by overcoming the challenges imposed by the environmental and operational variations.

In the feature extraction stage was detected the existence of unusual oscillations in the first three natural frequencies. These oscillations were found to be a result of the ambient temperature levels below 0°C, which caused a tremendous increase in the stiffness of the asphalt layer, resulting in large variations of the natural frequencies of the structure. By plotting the different natural frequencies versus temperature, a bilinear behavior with slop change around 0°C was discovered. In light of this discovery, a normality test was performed, unveiling that the natural frequencies in fact did not follow a multivariate normal distribution, rather it gave suggestions that the natural frequencies could follow a mixture of normal distributions. In the statistical modeling for feature classification stage, that fact was pointed out by the MSD-based algorithm, especially due to the concerning high level of false alarms. As a result and, in order to improve the feature classification performance, an algorithm based on the GMM was proposed.

In order to point out the influence of feature dimensionality for damage detection, two separate studies were performed by varying the dimension of the feature vectors. Firstly, assuming feature vectors composed by the three natural frequencies, the comparison of the results from the GMMs with the ones obtained assuming a unique multivariate normal distribution, showed a drop rate in terms of misclassifications of more than 50%, proving that the multivariate GMM was far more capable of differentiating changes caused by temperature variations from those changes caused by actual damage. Secondly, the same procedure was carried out by taking into account only the first two natural frequencies. In terms of total number of misclassifications, the results obtained were better than for the case of three natural

frequencies. However, the percentage of Type I errors, significantly lower than the assumed level of significance, suggested than the model with two natural frequencies was overfitted, and therefore not appropriate for general purposes.

Finally, comparing the MSD- and GMM-based algorithms, it is possible to conclude that the one based on a GMM has shown to be more appropriate under severe changes caused by operational and environmental variability, especially when those changes impose a non-linear structural response.

By reviewing Chapters 4 and 5, the difficulties undergone when analyzing data from a real-world bridge opposed to a laboratory structure become clear. In fact, the effects of the environmental conditions on the Z24 Bridge reinforce the fact that field deployment of SHM systems needs to be accompanied by robust techniques to take them into account in the damage identification process. The environmental and operational effects often have a large influence on the measured dynamics response of a structure and, as it was explained before, damage detection is based on the premise that damage in the structure will cause changes in the materials and, consequently, causing changes in measured vibration data. Therefore, it is crucial to quantify the effects of changing environmental and operational conditions so that they cannot hide little changes in the system's vibration signal caused by damage. Additionally, it important to create better and more reliable algorithms to extract damage-sensitive features, that are sensitive to damage and insensitive to operational and environmental changes, and to classify features despite the presence of operational and environmental changes.

Despite all the present challenges and limitations, the SHM field has had remarkable progresses throughout the years. Monitoring systems are able to recognize that the "patient" is sick and, furthermore, isolate the location and reason of the "illness". Monitoring systems have the ability to acquire, transmit and analyze data, and then to make decisions based on the relevant information derived from. The transition from time-based maintenance to a condition-based, where maintenance is scheduled based on the current state of the structure, is also a noteworthy step, reducing the considerable downtime due to current maintenance measures resulting in tremendous efficiencies in terms of cost. In the near future, the use of proper SHM systems could also allow further understanding of a structure's response through data analysis, which in turn could lead to better design methods. The SHM is a vast field and major breakthroughs are expected over the next few years due to recent investments and demands from bridge owners.

However, in order to transit SHM technology from research to practice, some issues still need to be addressed:

- a big difference between the lifespan of a bridge and the lifespan of a data acquisition system still exists; these systems are often under the same environmental conditions as the bridge, however they are far more susceptible to damage and degradation than the bridge itself; it is important that, for long term monitoring, durable and reliable hardware can be developed and successfully implemented at lower costs;

- the ability to detect damage on structures under varying operational and environmental conditions is still underdeveloped; better and more reliable algorithms are needed to extract damage-sensitive features that are sensitive to damage and insensitive to operational and environmental changes as well as to classify those features;

- SHM systems need to be viewed like any integral part of a bridge and, therefore, be included since the design project; only by thinking of bridge and monitoring system as a whole can a SHM system be entirely implemented into a structure.

Finally, in the years ahead, more real-world deployments should be carried out to further prove the applicability of the SHM technology to support the maintenance process. Nevertheless, the SHM is a vast field and major breakthroughs are expected over the next few years due to recent investments and demands from the bridge owners.

REFERENCES

1. Farrar C. and Wooden K. (2007), *An Introduction to Structural Health Monitoring*, Philosophical Transactions of the Royal Society, 365, 303-315.

2. Figueiredo, E. (2010), *Damage Identification in Civil Engineering Infrastructure under Operational and Environmental Conditions*, Doctor of Philosophy Dissertation in Civil Engineering, University of Porto, Faculty of Engineering.

3. Peeters, B., & De Roeck, G. (2001). *One-year Monitoring of the Z24-Bridge: Environmental Effects versus Damage Events*. Earthquake Engineering and Structural Dynamics, 30, 149-171.

4. Figueiredo, E., Park, G., Figueiras, J., Farrar, C., Worden, K. (2009*). Structural Health Monitoring Algorithm Comparisons using Standard Datasets*. Los Alamos National Laboratory Report: LA-14393.

5. Rytter, A. (1993). *Vibration Based on Inspections of Civil Engineering Structures*. PhD Dissertation, Department of Building Technology and Structural Engineering, Alborg University, Denmark.

6. About.com, Tourist Attractions in Chaves, Image retrieved August 27, 2012, from http://goeurope.about.com/od/chavesportugal/ss/chaves_pics_2.htm.

7. Carlos Santinho H., Freire L.R. (2012), The Implementation of a Bridge Maintenance Management System, proceedings of the IABMAS2012.

8. Wenzel H., 2009, *Health Monitoring of Bridges*, John Wiley & Sons, Ltd.

9. Khan M. (2010), *Bridge and Highway Structure Rehabilitation and Repair*, McGraw-Hill Companies, Inc.

10. Tampabay.com, Image retrieved November 5, 2011 from: http://www.tampabay.com

11. GenDisasters.com, Intersatete Bridge Collapse. Image retrieved November 3, 2011, from: http://www3.gendisasters.com/oklahoma/18589/webbers-falls-ok-interstate-bridge-collapse-may-2002

12. Silver Bridge Collapse. Accessed November 6, 2011: http://35wbridge.pbworks.com/w/page/900751/Silver%20Bridge%20Collapse

13. The Collapse of the Silver Bridge: NBS Determines Cause. Accessed November 6, 2011: http://museum.nist.gov/exhibits/silverbridge/index.htm

14. Mianus River Bridge Collapse. Accessed November 13, 2011: http://35wbridge.pbworks.com/w/page/900718/Mianus%20River%20Bridge%20Collapse

15. Schoharie Creek Thruway Bridge Collapse. Accessed December 11, 2011: http://35wbridge.pbworks.com/w/page/900747/Schoharie%20Creek%20Thruway%20Bridge%20Collapse

16. Schoharie Creek Thruway Bridge Collapse. Image retrieved December 11, 2011 from: http://35wbridge.pbworks.com/w/page/900747/Schoharie%20Creek%20Thruway%20Bridge%20Collapse

17. Overview of Bridge Inspection Programs (BIRM). Accessed December 11, 2011 from: http://www.cedengineering.com/upload/Bridge%20Inspection%20Programs.pdf

18. Settlement reached in Minnesota bridge collapse case. Image retrieved November 13, 2011: http://edition.cnn.com/2010/US/08/23/minnesota.bridge.settlement/index.html

19. Interstate 35W Mississippi River Bridge Fact Sheet. Minnesota Department of Transportation. Accessed November 13, 2011: http://www.dot.state.mn.us/i35wbridge/pdfs/factsheet.pdf

20. Time Photos. The Worst Bridge Collapses in the Past 100 Years. Accessed December 19. 2011: http://www.time.com/time/photogallery/0,29307,1649646_1421726,00.html

21. China Whisper. Unnatural Deaths of China Bridges. Accessed December 19, 2011: http://www.chinawhisper.com/unnatural-deaths-of-china-bridges

22. Echinacities. Bridge in Changchun Suddenly Collapses and Truck Falls into River. Accessed December 19, 2011: http://www.echinacities.com/in-pictures/1492_1.html#pic

23. Google Pictures. Retrieved November 5, 2011, from: http://nogabinete.blogspot.com/2011/03/como-e-da-natureza-das-coisas-culpa.html

24. Estradas de Portugal. S.A. Retrieved November 5, 2011, from: http://www.estradasdeportugal.pt/index.php/pt/imprensa/530-seminario-a-conservacao-do-patrimonio-de-obras-de-arte-da-ep

25. Failure Knowledge Database / 100 Selected Cases. Collapse of the Korea Seoul Seongsu Bridge. Accessed February 1, 2012 from: http://www.sozogaku.com/fkd/en/hfen/HD1000144.pdf

26. Civil Engineering Portal. Civil Engineering Disasters – Collapse of Bridges. Accessed February 1, 2012 from: http://www.engineeringcivil.com/theory/civil-engineering-disasters/page/2

27. Lauridsen, J., & Lassen, B. (1999). The Danish Bridge Management System DANBRO. In P. C. Das, *Management of Highway Structures* (pp. 61-70). Thomas Telford Publishing.

28. Mendonça, T. P., & Vieira, A. (2004). Bridge Management System - GOA. *Proceedings of the 2nd International Conference of the International Association for Bridge Maintenance and Safety*. 18-22 October, Kyoto, Japan: Routledge USA.

29. Poças, R. F. G. (2009), Gestão do Ciclo de Vida de Pontes. MSc dissertation, Universidade do Minho.

30. Walther, R. A., & Chase, S. B. (2006). *Condition Assessment of Highway Structures: Past, Present, and Future*. Transportation Research Circular - 50 Years of Interstate Structures: Past, Present, and Future (E-C104), 67-78.

31. Inaudi, D. (2009). *Integrated Structural Health Monitoring Systems of Bridges.* ASCP'09 – 1º Congresso de Segurança e Conservação de Pontes ASCP, 2-3 de Julho 2009, Lisboa, Portugal.

32. Case Study – Bridges. Structural monitoring of the Manhattan cable stayed bridge. Accessed January 22, 2012 from: http://www.micronoptics.com/

33. Peterson B., (2010) *The Rehabilitation Alternative Huey P. Long Bridge Case Study.* Bridge Engineering Distinguished Speaker Series, MCEER.

34. Boller C., Chang F.., Fujini Y. (2009) *Encyclopedia of Structural Health Monitoring*, John Wiley & Sons, Ltd. ISBN: 978-0-470-05822-0.

35. Ponte da Lezíria sobre o Rio Tejo, NewMENSUS, Lda. Accessed February 2, 2012: http://www.newmensus.pt/projectos.php

36. McLinn, J. (2009) Major bridge collapses in the US, and around the world. IEEE Reliability Society 2009 Annual Technology Report.

37. Glisic, B., Inaudi, D., Casanova, N. (2010) *SHM process as perceived through 350 projects.* SPIE conference on Smart Structures and NDE, San Diego, California, USA.

38. Figueiredo, E. (2006), *Monitorização e Avaliação do Comportamento de Obras de Arte*, Tese de Mestrado, Faculdade de Engenharia da Universidade do Porto, Portugal.

39. Farrar C., Sohn H., Doebling S. (2000), *Structural Health Monitoring At Los Alamos National Laboratory.* Los Alamos National Laboratory: MS P-946.

40. Sohn H., Farrar C., Hemez F., Shunk D., Stinemates D., Nadler B., et al. (2004). *A Review of Structural Health Monitoring Literature from 1996-2001.* Los Alamos National Laboratory: LA-13976-MS.

41. Figueiredo, E., Park, G., Farrar, C. R., Worden, K., Figueiras, J. (2011). *Machine Learning Algorithms for Damage Detection under Operational and Environmental Variability*. International Journal of Structural Health Monitoring, 10(6), 559-572.

42. Alampalli, S. (1998) *Influence of in-service environment on modal parameters.* In Proc. IMAC XVI, Santa Barbara, CA, pp. 111-116.

43. Kim, C.-Y., Jung, D.-S., Kim, N.-S., Kwon, S.-D., & Feng, M. Q. (2003). Effect of Vehicle Weight on Natural Frequencies of Bridges Measured from Traffic-induced Vibration. *Earthquake Engineering and Engineering Vibration*, 2 (1), 109-115.

44. Sensorland. Accessed February 6, 2012 from: http://www.sensorland.com/

45. Image retrieved February 6, 2012 from: http://www.stanford.edu/class/me220/data/lectures/lect10/lect_6.html

46.Wikipedia the Free Encyclopedia. Image retrieved February 6, 2012, from: http://en.wikipedia.org/wiki/Linear_variable_differential_transformer

47. A-Tech Instruments Ltd. Image retrieved February 6, 2012, from: http://www.a-tech.ca/subcat.php?id=16

48. Farrar C., Sohn H. (2000), *Pattern Recognition for Structural Health Monitoring.* Los Alamos National Laboratory, Los Alamos, NM 87545, MS P-946.

49. Box, G. E., Jenkins, G. M., & Reinsel, G. C. (1994). *Time Series Analysis: Forecasting and Control* (3rd Edition ed.). New Jersey: Prentice-Hall, Inc.

50. Figueiredo, E.; Park, G.; Figueiras, J.; Farrar, C.; Worden, K. (2011). *Influence of the Autoregressive Model Order on Damage Detection*. Computer-Aided Civil and Infrastructure Engineering, 26 (3), 225-238.

51. Farrar C., Duffey T., Doebling S., Nix D. (1999), *A Statistical Pattern Recognition Paradigm for Vibration-Based Structural Health Monitoring*. 2nd International Workshop on Structural Health Monitoring, Stanford, CA.

52. Figueiredo, E., Park, G., Figueiras, J., Farrar, C., Worden, K. (2009), *Structural Health Monitoring Algorithm Comparisons Using Standard Data Sets.* Los Alamos National Laboratory, Los Alamos, LA-14393.

53. Reynolds D. (2008), *Gaussian Mixture Models*. Encyclopedia of Biometric Recognition, Springer, Journal Article, February 2008.

54. Figueiredo, E.; Radu, L.; Westgate, R.; Brownjohn, J.; Cross, E.; Worden, K.; and Farrar, C. (2012). Applicability of a Markov-chain Monte Carlo Method for Damage Detection on Data from the Z-24 and Tamar Bridges. Proceedings of the 6th Workshop on Structural Health Monitoring, July 3-6, Dresden, Germany.

55. Figueiredo, E., Radu, L., Park, G., Farrar, C. R., Figueiras, J. (2011). An Approach to Integrate Structural Health Monitoring with Bridge Management Systems. Proceedings of the *International Conference on Structural Engineering Dynamics*, 20-22 June, Tavira, Portugal.

56. Flynn, E. B.; Kpotufe, S.; Harvey, D.; Figueiredo, E.; Taylor, S.; Dondi, D.; Mollov, T; Todd, M. D.; Rosing, S. T.; Park, G.; Farrar, C.R. (2010). SHMTools: A New Embeddable Software Package for SHM Applications. *SPIE Smart Structures and Materials + Nondestructive Evaluation, 764717*, 7-11 March, San Diego, CA, USA.

57. Peeters B.(2000), *System Identification and Damage Detection in Civil Engineering*. PhD thesis, Department of Civil Engineering, Katholieke Universiteit Leuven, Belgium, 2000.

58. Peeters B., Maeck J., De Roeck G. (2000) *Dynamic Monitoring of the Z24 Bridge: Separating Temperature Effects from Damage*. In Proceedings of the European COST F3 Conference on System Identification and Structural Health Monitoring, Madrid, Spain, June 2000, 377-386.

59. Steenackers G., Guillaume P. (2005) *Structural health monitoring of the Z24 bridge in presence of environmental changes using modal analysis.*In 23rd Int. Modal Analysis Conf, Orlando, FL., Jan.2005.

60. Figueiredo, E.; Radu, L.; Westgate, R.; Brownjohn, J.; Cross, E.; Worden, K.; and Farrar, C. (2012). Applicability of a Markov-chain Monte Carlo Method for Damage Detection on Data from the Z-24 and Tamar Bridges. Proceedings of the 6th Workshop on Structural Health Monitoring, July 3-6, Dresden, Germany.

61. Figueiredo, E.; Radu, L.; Park, G.; Farrar, C. R. (2011). Integration of SHM into Bridge Management Systems: Case Study – Z24 Bridge. Proceedings of the *8th International Workshop on Structural Health Monitoring*, 13-15 September, Palo Alto, CA, USA.